Studies on Structure and Activity of Advanced Titanium Oxide Photocatalyst

(高機能化した酸化チタン光触媒の構造と活性に関する研究)

Shinichi KAWASAKI

河崎　眞一

2008

Studies on Structure and Activity of Advanced Titanium Oxide Photocatalyst
(高機能化した酸化チタン光触媒の構造と活性に関する研究)

Shinichi KAWASAKI

河崎　眞一

2008

Contents

Acknowledgements

List of Publications

Chapter 1

General Introduction

1. 1 Introduction to TiO_2 photocatalytic reactions

Titanium oxides with a crystal structure of anatase or rutile produce an exited pair of electrons and a positive hole upon ultra violet (UV) light irradiation. The exited electron and positive hole allow reduction and oxidation reactions to proceed in a variety of materials. Such reactions employing titanium oxide catalysts are commonly photo-oxidative ones involving active oxygen species. Among active oxygen species, atomic oxygen plays a crucial role in the photo-oxidative reactions. Specifically, an oxygen molecule adsorbed on a titanium oxide catalyst accepts the exited electron from the titanium oxide catalyst to produce an O_2^- radical, and then a positive hole reacts with the O_2^- radical to produce two oxygen atoms. Then, immediately after the production of the exited electron and positive hole, these separately move to different surface sites on the titanium oxide catalyst. Thus, the recombination of the electron and positive hole is suppressed.

On the other hand, isolated titanium oxide species are produced by such methods as ion-exchange and chemical vapor deposition. Isolated titanium oxide species are commonly loaded in a highly dispersed state on a support made up of oxides. Highly dispersed isolated titanium oxide species possess unique coordination structures and reflect the structure of the support. The local structures of anatase and rutile have hexagonal-coordinations of oxygen. The isolated titanium oxide species, however, has a tetrahedral-coordination of oxygen [1]. This difference of

structures may cause unique differences in their photoreactive mechanisms. The isolated titanium oxide species have peculiarly high catalytic activity for photoreactions and facilitate the reduction of even carbon dioxide in the presence of water under UV irradiation [2-3]. It is becoming clear that such photocatalytic reactions involve a charge transfer between reactants and an excited triplet state of the isolated titanium oxide species as distinct from a normal photo-oxidative reaction [4-8]. In the excited triplet state of the isolated titanium oxide species, the exited electron and a positive hole do not separately act, but coexist in very close proximity. This feature of the electrons and a positive hole is strongly related to the photo-reactions on the isolated titanium oxide species that can not be observed for the anatase or rutile structured titanium dioxide powders.

1. 2 Purpose of this study

It is very possible that an isolated titanium oxide species loaded on the inner wall of a porous support shows increased selectivity in photocatalytic reactions. Designing a photocatalyst in a space in micropores or mesopores means the photocatalyst will be smaller than the space. The size of the photocatalyst thus will be from several nanometers to tens of nanometers. The structure of this kind of highly fine titanium oxide species depends on the structure of the supports and, therefore, can be easily controlled to demonstrate high selectivity in various photoreactions. When using zeolites as the support, the titanium oxide incorporated therein

shows different selectivities that are dependent on the type of the pore structure [9-12].

In most methods for the preparation of isolated titanium oxide species, however, the synthesis processes are complicated. For example, when the amount of the titanium oxide species loading increases, dispersibility of the titanium oxide species on the support decreases. Thus, the design of a photocatalyst having an active controlled site is difficult.

Contrary to the above, using a sol-gel method easily produces homogeneous inorganic materials at low temperatures. The sol-gel method uses metal alkoxides as starting materials for the production of composite oxides. By changing the amounts of the starting materials, the composition of the oxide can be easily controlled. Further, the sol-gel method is suitable for the formation of a variety of types of catalysts such as thin film catalysts.

In this study, a series of Ti/Si binary oxide catalysts having a variety of compositions were prepared using the sol-gel method. Characterization of the catalysts was carried out and their photocatalytic activities investigated. Next, many types of isolated titanium oxide species were prepared and compared in terms of their photocatalytic activities in photosynthetic reductions of CO_2 with H_2O.

With the aim of designing a photocatalyst composed of titanium oxide that had high selectivity, isolated titanium oxide species were incorporated in the structure of β-zeolite or loaded on mesoporous silica. The effects of surface modification using fluorine atoms on the chemical or

physical properties of the titanium oxide species and on their photocatalytic activities were then investigated.

As well, TiO_2 fine particles were synthesized and modified with fluorine atoms to improve the photocatalytic activity for the degradation of organic pollutants and toxicants.

1. 3 References

[1] J. M. Thomas and G. Sankar, *J. Synchrotron Radiat.*, 8, 55 (2001).

[2] H. Yamashita and M. Anpo, *Curr. Opin. Solid State Mater. Sci.*, 7, 471 (2004).

[3] O. Ishitani, C. Inoue, Y. Suzuki, T. Ibusuki, *J. Photo-chem. Photobiol. A: Chem.*, 72, 269 (1993).

[4] M. Anpo and M. Sunamoto, *Kougyo Zairyo*, 37, 56 (1989).

[5] M. Anpo, *Hyomen Kagaku*, **11**, 39 (1990).

[6] M. Anpo, M. Matsuoka, Y. Shioya, H. Yamashita, E. Giamello, M. Che, M. A. Fox, *J. Phys. Chem.*, 98, 5744 (1994).

[7] H. Yamashita, M. Matsuoka, Y. Shioya, M. Anpo, "Science and Technology in Catalysis 1994" Kodansya, Tokyo, 227 (1995).

[8] H. Yamashita, Y. Ichihashi, M. Anpo, *Hyomen*, 16, 194 (1995).

[9] M, Anpo, M. Kondo, S. Coluccia, C. Louis, M. Che, *J. Am. Chem. Soc.*, 111, 8791 (1989).

[10] M. Anpo and K. Chiba, *J. Mol. Catal.*, 74, 207 (1992).

[11] H. Yamashita, A. Shiga, M. Anpo, Proc. JAPAN-FSU Catal. Seminar, 88

(1994).

[12] H. Yamashita, S. Kawasaki, M. Anpo, *Shokubai*, **36**, 440 (1994).

Chapter 2

Characterization of Titanium-Silicon Binary Oxide Catalysts Prepared by the Sol-Gel Method and Their Photocatalytic Properties:

(1) The Liquid-Phase Oxidation of 1-Octanol

(2) The Hydrogenation and Hydrogenolysis of CH_3CCH with H_2O

2. 1 Introduction

Titanium oxide catalysts have attracted a great deal of attention as potential photocatalysts to address urgent and global environmental concerns [1-4]. The photocatalytic degradation of various toxic compounds in aqueous solutions using fine titanium oxide particles has been studied by many researchers [5-10]. However, to avoid the filtration and suspension of small photocatalyst particles, the design of highly efficient and transparent titanium oxide photocatalyst is strongly desired. The preparation of titanium oxide catalysts on transparent supports such as Vycor glass by anchoring or embedding methods can be considered one of the most promising ways to achieve such applicable photocatalysts [10].

Anpo et. al. have reported that titanium oxide having a tetrahedral coordination can be chemically supported onto transparent Vycor glass by the chemical vapor deposition or anchoring method and have shown that such catalysts exhibit high and characteristic photocatalytic reactivities [11-13]. Conventionally, highly dispersed titanium oxides included within the zeolite cavities and framework have been prepared as tetrahedral titanium oxide species using an ion-exchange method or hydrothermal synthesis and used as efficient photocatalysts for various photocatalytic reactions such as the decomposition of NOx into N_2 and O_2 [14-16]. These findings clearly suggest that highly dispersed tetrahedral titanium oxide catalysts exhibit unique and efficient reactivity for various gas-phase photocatalytic reactions compared to bulk TiO_2 powder catalysts.

The sol-gel process is expected to offer unique advantages for the preparation of such highly dispersed tetrahedrally coordinated and transparent photocatalysts especially to be applied for coating material, active thin-film photocatalysts, and multi-component ceramics [17-19]. For binary oxide catalysts, the local structure of the active sites as well as the catalytic and photocatalytic properties are strongly dependent on the composition of the oxides [19]. Therefore, it is of special interest to investigate the relationship between the local structure of the titanium oxide species and the photocatalytic reactivity of the Ti/Si binary oxides prepared by the sol-gel method as a function of the Ti content. In fact, Anpo et al. have reported that the photocatalytic reactivities of the Ti/Si binary oxides prepared by the coprecipitation method are affected by changing the composition of the catalyst [20]. Imamura et al. have reported that the Ti/Si binary oxides prepared by the sol-gel method exhibit a high catalytic activity for the selective epoxidation of alkenes [21], while Davis et al. have investigated the local structure of the titanium oxide species in the Ti/Si binary oxide using XAFS techniques [22-23]. However, there have been few detailed investigations not only on the characterization of the catalysts at the molecular level but also on the role the local structure of the active sites plays on the photocatalytic reactivities of such Ti/Si binary oxide catalysts.

In the present study, the authors deal with the preparation of highly active tetrahedral titanium oxide species embedded into transparent SiO_2 matrixes using the sol-gel method and have carried out a comprehensive

characterization of these catalysts by means of photoluminescence, UV-vis reflectance, FT-IR, ESR, XAFS, XPS, and XRD spectroscopic techniques. These Ti/Si binary oxide catalysts have also been successfully applied as photocatalysts for the liquid-phase oxidation of 1-octanal to produce 1-octanal at 300 K in an acetonitrile solution. Special attention has been focused on the relationship between the local structure of the titanium oxide species in the Ti/Si binary oxides and the photocatalytic reactivity in order to provide vital information for the design and application of such highly efficient phoyocatalytic system in the degradation of toxic compounds diluted in a liquid phase.

Further, we have clarified the relationship between the local structure of the titanium oxide species and the photocatalytic properties in the hydrogenation and hydrogenolysis of CH_3CCH with H_2O. In addition, the effects of addition of Pt on the photocatalytic properties has been studied in order to obtain useful and important information required for the design and application of highly active and selective photocatalytic systems.

2. 2 Experimental

2. 2. 1 Catalysts

Tetraethyl orthosilicate (TEOS, 99%), titanium isopropoxide (TPOT, 99%), and ethanol (99.5%) were supplied by Kishida Chemicals, Japan, and used as received. Titanium silicon (Ti/Si) binary oxides having different Ti contents were prepared by the sol-gel method from ethanol solution of

mixtures of tetraethyl orthosilicate (TEOS) and titanium isopropoxide (TPOT). These starting ethanol solutions were prepared from ethanol (20 mL) and the mixtures (20 mL) of TEOS and TPOT. These solutions were kept in a sealed container under the air of the saturated moisture which was kept in the storage room controlled at the room temperature of 296 ± 1 K. Thus, the gelation of mixtures of TEOS and TPOT in ethanol solution was carried out under mild conditions using the saturated moisture (21 ± 2 mmHg) of the air at 296 ± 1 K without the addition of any other reagents. The gelation proceeded slowly and was completed within 7-15 days, forming the homogeneous Ti/Si gel samples. The period required for completing the gelation depended on the composition of the starting mixtures. Aging and drying of the gel samples leading to the transformation from gel to xerogel were carried out by allowing the samples to stand under the same conditions for an extra 4 weeks. These xerogel samples were transparent and seemed to have a homogeneous composition without any segregation. The Ti/Si xerogel formed this way were crushed and sieved to 0.25 mm size particles and washed with sufficient amounts of boiled water. Calcination of the Ti/Si xerogel samples was carried out in dry air at 725 K for 5 h to produce stable Ti/Si binary oxide catalysts.

The Pt-loaded Ti/Si binary oxide catalyst (1.0 wt % as Pt metal) was prepared by impregnating the binary oxide with an aqueous solution of H_2PtCl_6.

Prior to the spectroscopic measurements and photocatalytic reactions, these binary oxide catalysts were treated with oxygen at 725 K

for 2 h and evacuated at 475 K for 2 h to remove any organic contaminants adsorbed on the catalysts to obtain clean surfaces and the reproducible photocatalytic properties.

2. 2. 2 Characterization

The photoluminescence spectra of the catalyst were measured at 77 K using a Shimadzu RF-5000 spectrophotofluorometer. The Uv-vis absorption spectra were measured at 295 K by a Shimadzu UV-2200A double-beam digital spectrophotometer equipped with conventional components of a reflectance spectrometer. The FT-IR spectra were recorded at 295 K with a Shimadzu FTIR-8500 spectrophotometer using the sample wafers of mixture of catalyst and KBr. X-ray diffraction patterns of the catalysts were obtained with a Rigaku RD-γA X-ray diffractometer using CuKα radiation with a Ni filter. ESR spectra were recorded at 77 K using a JEOL JES-RE2X spectrometer operating in the X-band mode. The XPS spectra were measured at 295 K with V.G. Scientific ESCASCOPE photoelectron spectrometer using Mg Kα radiation. The XAFS spectra (XANES and EXAFS) of the catalysts were measured at the BL-7C facility of the Photon Factory at the National Laboratory for High-energy Physics, Tsukuba. Si (111) double crystals were used to monochromatize the X-rays from the 2.5 GeV electron storage ring. The Ti K-edge absorption spectra were recorded in the transmission mode or fluorescence mode at 295 K. The normalized spectra were obtained by a procedure described in previous literature [24], and Fourier transformation was performed on κ^3-weighted

EXAFS oscillations in the range 3 - 10 $Å^{-1}$. The curve-fitting of the EXAFS data was carried out by employing the iterative nonlinear least-squares method and empirical backscattering parameter sets extracted from the shell features of titanium compounds.

2. 2. 3 Photocatalytic Reactuions

2. 2. 3. 1 Liquid-Phase Oxidation of 1-Octanol

The catalyst (50 mg) was preheated in dry air at 725 K and cooled to room temperature before being placed with 1-octanol (0.5 mmol) in a volumetric flask (25 mL) which was then filled with acetonitrile. The sample was then transferred to a quartz test tube (30 mm i.d.) and sealed with a rubber septum. Oxygen was bubbled through a Teflon tube (1 mm i.d.), and the sample was irradiated at 300 K with vigorous and continuous stirring in a Rayonet photochemical reactor (Southern New England Ultraviolet) [13]. A phosphor-coated low-pressure mercury lamp, RPR-3000 (blazed at about 300 nm), was used as the excitation source. The products were analyzed on a Hewlett-Packard model 5890 gas chromatograph equipped with an Alltech capillary column (0.25mm×25 m).

2. 2. 3. 2 Hydrogenation and Hydrogenolysis of CH_3CCH with H_2O

The catalyst was treated with O_2 at 725 K for 2 h and then evacuated for 2 h at 475 K. In the case of Pt-loaded catalysts, the pretreated catalyst was heated in H_2 at 475 K for 2 h and finally evacuated

at the same temperature. The catalyst (150 mg) was spread out evenly on the flat bottom of the quartz cell. UV irradiation of the catalyst in the presence of CH_3CCH (11 μ mol) and gaseous H_2O (54 μ mol) was carried out using a 75-W high pressure Hg lamp through water and color filters (λ >290 nm) at 275 K. The reaction products collected in the gas phase were analyzed by gas chromatography.

2. 3 Results and Discussion

The crystalline structures of Ti/Si binary oxides having different Ti contents were investigated by XRD measurements. The XRD patterns obtained are shown in Figure 2-1. The XRD patterns of the binary oxides exhibit only diffraction lines that are attributed to the crystalline anatase phase of TiO_2. The sizes of the crystallites measured by peak half-width were 115 and 67 Å with the TS-100 and TS-80 samples, respectively. The very weak diffraction line assigned to the crystalline brookite phase of TiO_2 could be observed only with TS-100 sample.

When the Ti content decreased, these X-ray diffraction lines decrease in intensity and finally disappear. This indicates that, in the Ti/Si binary oxides, the crystallinity of the titanium oxide species decreases when the Ti content is decreased. Especially, in the binary titanium oxide having Ti contents lower than 50 wt % TiO_2 the titanium oxide species are present in amorphous structure within the SiO_2 matrixes.

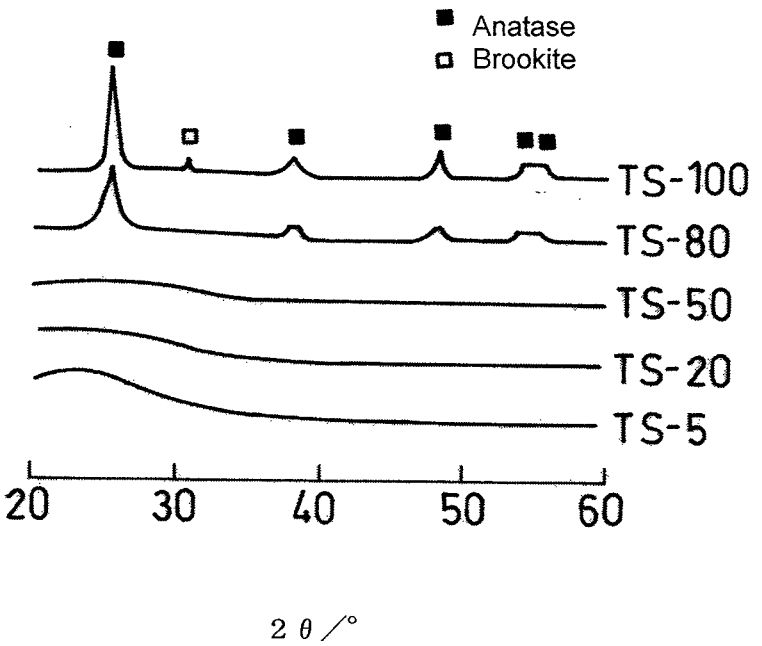

Figure 2-1. X-ray diffraction patterns of Ti/Si binary oxides. Ti/Si binary oxides having a Ti content of 5 and 80 wt % TiO_2 are referred to as TS-5 and TS-80, respectively, and the TS-100 sample is TiO_2 prepared by the sol-gel method.

Figure 2-2 shows the FT-IR spectra of Ti/Si binary oxides having different Ti contents. With these oxides, three characteristic bands can be observed at around 1100, 950, and 650 cm^{-1} [22-23]. SiO_2 and the Ti/Si binary oxide having a low Ti content exhibit a band at around 1100 cm^{-1} which can be assigned to the stretching of the Si-O-Si bond in the tetrahedral SiO_4 unit of the SiO_2 matrixes. TiO_2 and the binary oxide having a large Ti content exhibit a band at 650cm^{-1} which is representative of TiO_2 matrixes, while the Ti/Si binary oxides exhibit an additional bond at around 950 cm^{-1}. This band has been assigned to the stretching of the $Si\text{-}O^-$ species of Si-O-Ti or $Si\text{-}O^-$ defect sites which are formed by the

inclusion of Ti^{4+} ions the SiO_2 matrixes in the previous literature [23, 25]. Thus, the appearance of the band at around 950 cm^{-1} indicates that the titanium oxide species are embedded into SiO_2 matrixes within these Ti/Si binary oxides.

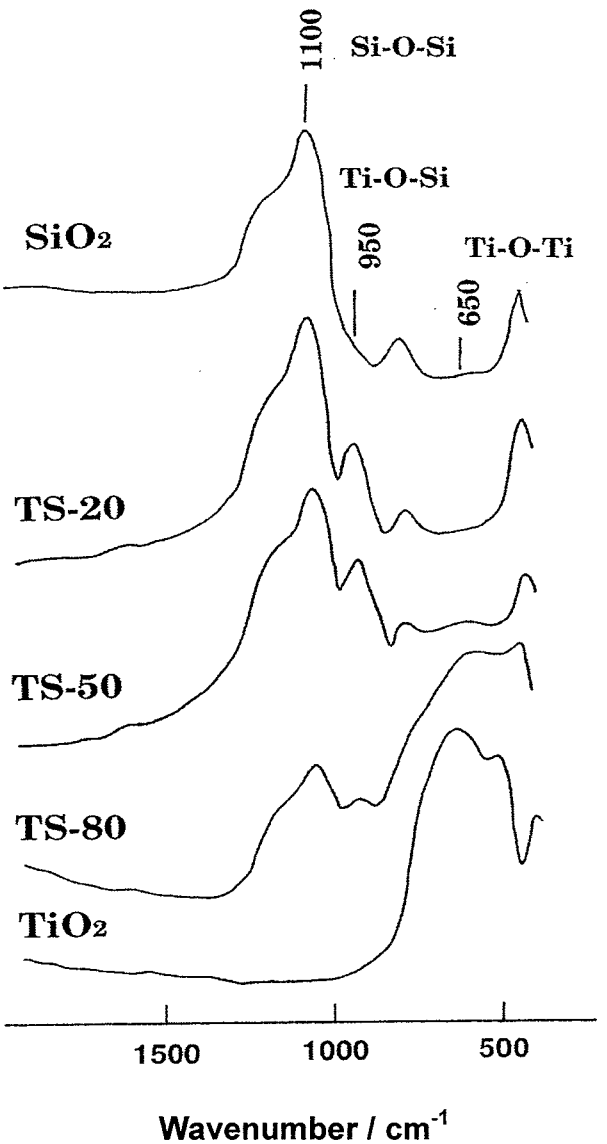

Figure 2-2. FT-IR spectra of Ti/Si binary oxides and powdered SiO_2 and TiO_2 (anatase). TS-20, TS-50, and TS80 samples are the Ti/Si binary oxides of 20, 50, and 80 wt % TiO_2, respectively.

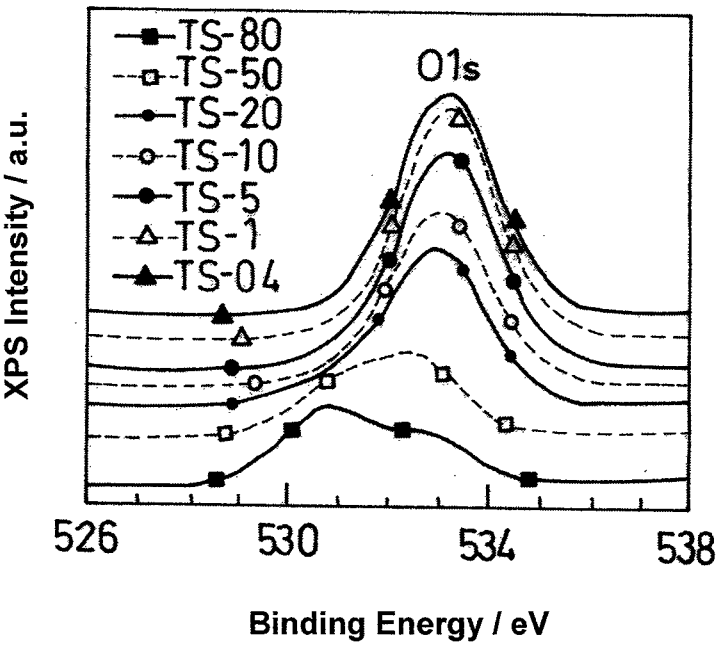

Figure 2-3. X-ray photoelectron spectra of the O 1s level for Ti/Si binary oxides. TS-0.4 - TS-80 samples are the Ti/Si binary oxides of 0.4 - 80 wt % TiO_2, respectively.

The XPS spectra of the catalysts were measured in order to obtain information on the binding energy of the titanium oxide species. Figure 2-3 shows the XPS spectra of the O1s band for Ti/Si binary oxides having different Ti contents. The band of the O ion in the TiO_2 matrixes (Ti-O-Ti) can be observed at around 530.5 eV, and that of the SiO_2 matrixes (Si-O-Si) can be observed at around 533.5 eV. With an increase in the Ti content of these Ti/Si binary oxides, the O1s peak shifts from 535.5 eV to a lower energy of around 532.5 eV. Stakheev and co-workers observed the same shift of the O1s band with a change in the Ti content of the Ti/Si binary oxides prepared by coprecipitation and concluded that this shifts reflects a substitution of the Si atoms by less electronegative and more polarizable Ti

atoms in the SiO_2 matrixes [26]. With the Ti/Si binary oxide having a Ti content of 50 - 80 wt% (TS-50, TS-80), the two O1s bands can be observed at around 530.5 and 532.5 eV. Considering the previous detailed XPS study on Ti/Si binary oxides [25], the appearance of these two bands indicates the formation of a two-phase system containing both a titania-rich phase and a phase in which the titanium oxide species are embedded into the SiO_2 matrixes, these results being in good agreement with the results of the FT-IR investigations.

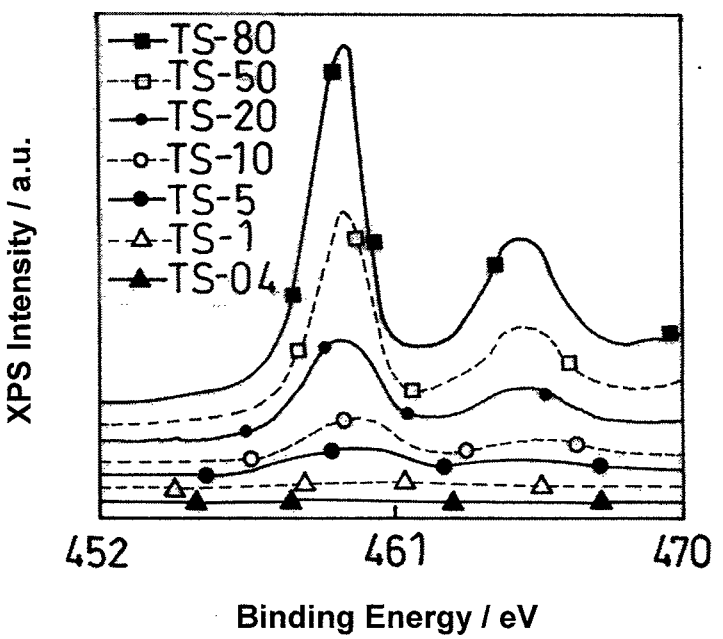

Figure 2-4. X-ray photoelectron spectra of the Ti2p levels for Ti/Si binary oxides. TS-0.4 - TS-80 samples are the Ti/Si binary oxides of 0.4 - 80 wt % TiO_2, respectively.

Figure 2-4 shows the XPS spectra of the Ti2p band for Ti/Si binary oxides having different Ti contents. The binding energy of the Ti($2p_{3/2}$) and

$Ti(2p_{1/2})$ bands shifts to higher values when the Ti content decreases, especially with binary oxides having less than 20 wt% TiO_2. A similar tendency has been observed for the $Ti(2p_{3/2})$ XPS signals of the Ti/Si and Ti/Al binary oxides prepared by coprecipitation [20, 27]. Taking these results into consideration, such a shift in the binding energy of the Ti2p bands to higher values can be attributed to the smaller relaxation energy for the highly dispersed titanium oxide species as compared to the powdered bulk TiO_2 catalysts.

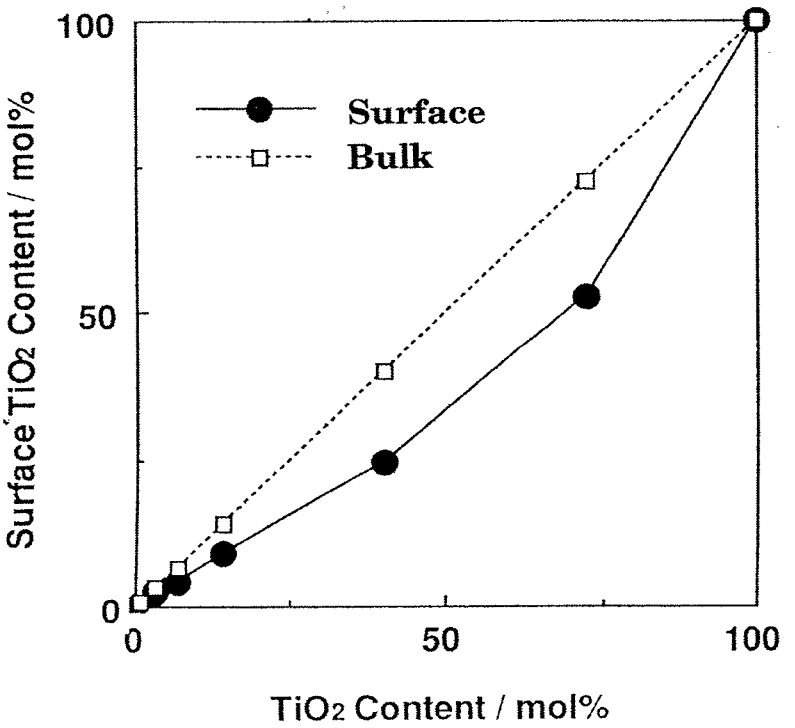

Figure 2-5. Surface Ti composition of Ti/Si binary oxides calculated from the signal intensity of $Ti(2p_{1/2})$ and $Si(2p_{1/2})$ XPS bands in the Ti/Si binary oxides. Dotted line: the surface Ti composition calculated from the results of XPS measurement. Bold line: the original composition of the sols (bulk Ti content).

Figure 2-5 shows the surface Ti composition of Ti/Si binary oxides calculated from the ratio of the $Ti(2p_{3/2})$ to $Si(2p_{1/2})$ XPS band intensities. It can clearly be seen that there is a steady decrease in the surface Ti composition as the bulk Ti content in the Ti/Si binary oxides decreases. However, the surface Ti composition is much smaller than what can be expected from the original composition of the sols region of middle Ti content of around 50 wt% TiO_2 suggesting the segregation of SiO_2 in the surface region of the binary oxides.

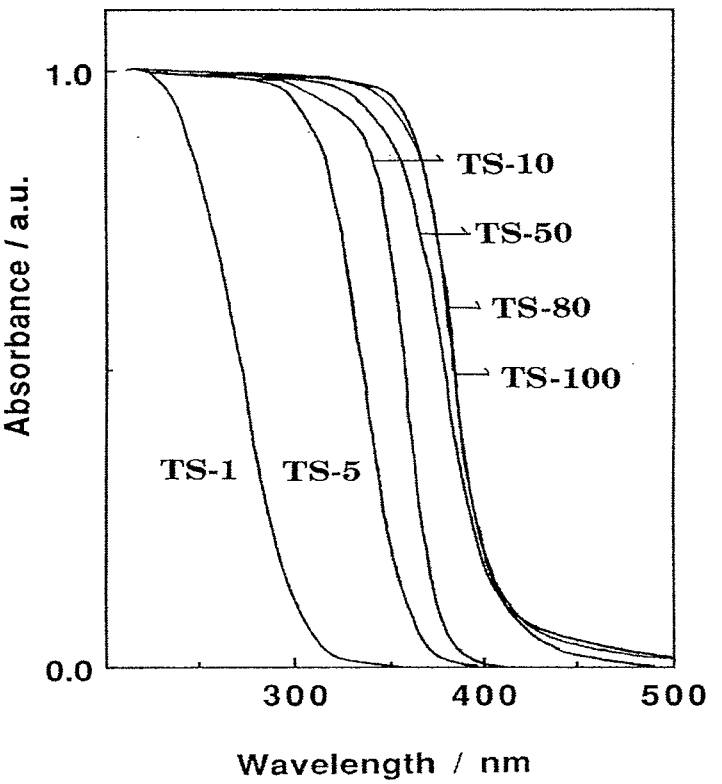

Figure 2-6. Absorption spectra of Ti/Si binary oxides measured by the UV-vis diffuse reflectance method. TS-1 - TS-80 samples are the Ti/Si binary oxides of 1 - 80 wt % TiO_2, respectively, and the TS-100 sample is TiO_2 prepared by the sol-gel method.

Figure 2-6 shows the absorption of Ti/Si binary oxides measured by the UV-vis diffuse reflectance method. It can be seen that a decrease in the Ti content causes a remarkable shift in the absorption band toward shorter wavelength regions. Similar studies were carried out on the Ti/Si and Ti/Al binary oxides having various compositions of Ti:Si and Ti:Al prepared by coprecipitation, and a considerable shift toward shorter wavelength regions was observed for the absorption band of the highly dispersed titanium oxide species [20, 27]. It can be said that such a large shift toward shorter wavelengths for the Ti/Si binary oxides with low Ti content is attributed to the size quantization effect arising from presence of extremely small titanium oxide particles and/or presence of highly dispersed titanium oxide species having a low coordination number. These results obtained by XRD, XPS, and UV-vis absorption measurements clearly show that a decrease in the Ti content changes the crystalline structure of the titanium oxides from aggregates in an anatase phase to ultrafine titanium oxide species with an amorphous structure and eventually to isolated titanium oxide species having a local coordinate geometry different from those of the crystalline anatase titanium oxide, the extent of the transformation strongly depending on the Ti content.

Ti/Si binary oxide having a low Ti content of less than 20 wt% TiO_2 exhibited the characteristic photoluminescence spectra at around 490 nm when the catalysts were excited at around 280 nm. Figure 2-7 shows the typical photoluminescence spectra observed with Ti/Si binary oxides having a low Ti content by excitation at around 280 nm at 77 K. The observed

photoluminescence spectra are in good agreement with those of the highly dispersed tetrahedrally coordinated titanium oxides anchored onto Vycor glass where the absorption of UV light at around 280 nm brought about an electron transfer from the lattice oxygen (O_l^{2-}) to the titanium ion (Ti_l^{4+}) to from a charge transfer excited state, ($Ti^{3+} \cdot O^-$) [12-15]. These findings show that the observed photoluminescence spectrum is attributed to the radiative decay process from the thus formed charge-transfer excited state to the ground state of the highly dispersed titanium oxide species having a tetrahedral coordination. On the other hand, Ti/Si binary oxides having a large Ti concentration did not exhibit photoluminescence.

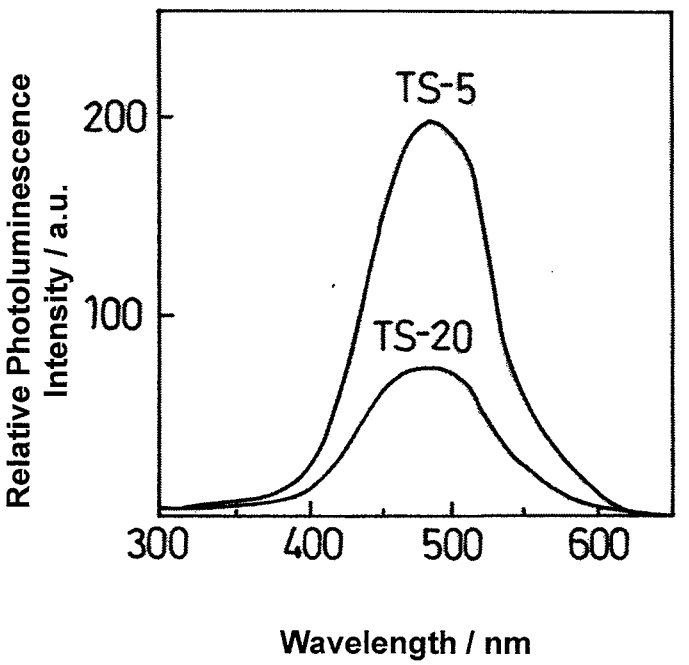

Figure 2-7. Photoluminescence spectra of Ti/Si binary oxides. TS-5 and TS-20 samples are the Ti/Si binary oxides of 5 and 20 wt % TiO_2, respectively. Photoluminescence spectra were measured at 77 K by the excitation at 280 nm.

Figure 2-8 shows the effect of the Ti content on the yield of the photoluminescence spectrum due to the presence of highly dispersed titanium oxide species in the Ti/Si binary oxides. Decreasing the Ti content led to an increase in the yield of the photoluminescence spectrum. At the same time, the band position shifted to the shorter wavelength regions. These findings indicate that such a decrease in the Ti content of the binary oxides causes the titanium oxides species to exist in a highly dispersed state with a low coordination in the SiO_2 matrixes.

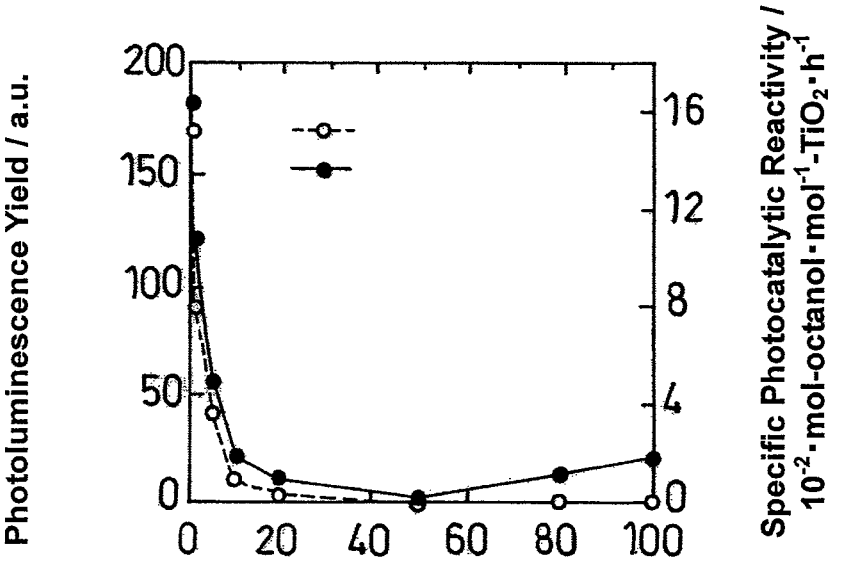

Figure 2-8. Specific intensity of the photoluminescence of Ti/Si binary oxides and their specific photocatalytic reactivities for the liquid-phase oxidation of 1-octanol to 1-octanal.

Similar phenomena can be observed for the Zr/Si binary oxide catalysts prepared by the sol-gel method in which a decrease in the Zr content caused the photoluminescence intensity to increase and its band

and position to shift to shorter wavelength regions, indicating that zirconium oxide species are highly dispersed in a state of coordinative unsaturation within the Zr/Si binary oxides [19].

Figure 2-9 shows the XANES spectra of Ti/Si binary oxides. The XANES spectra of the titanium oxide catalyst at the Ti K-edge show several well-defined pre-edge peaks which are related to the local structures surrounding the Ti atom, while the relative intensities of the pre-edge peaks also provide useful information on the coordination number [22, 28-31].

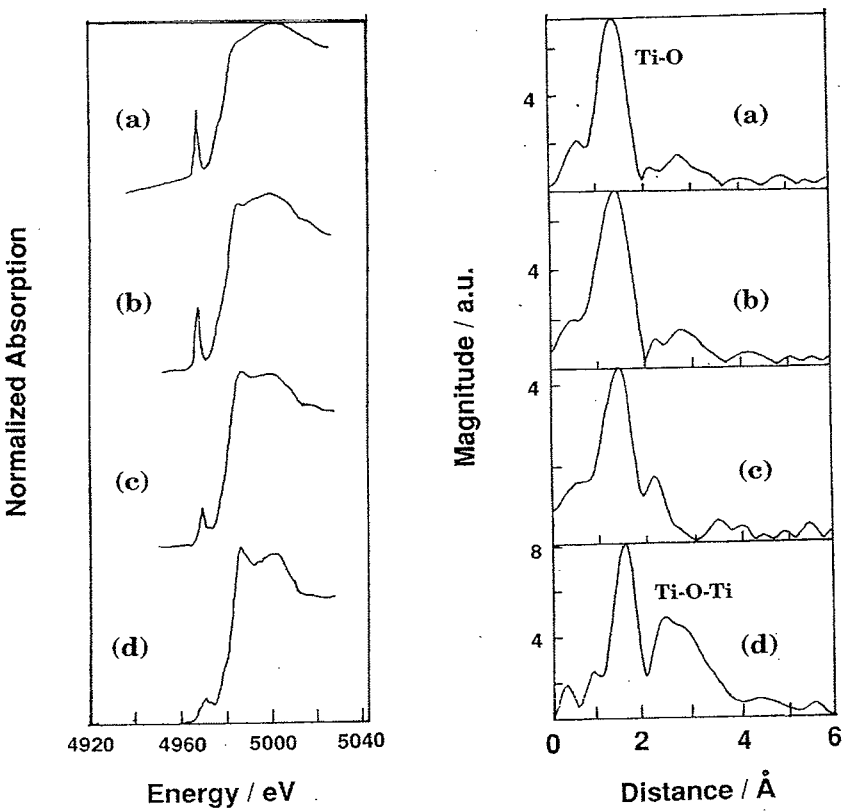

Figure 2-9. XANES (left) and Fourier transforms of EXAFS spectra (FT-EXAFS) (right) of Ti/Si binary oxides. Ti contents are (a) 1 wt % (TS-1), (b) 5 wt % (TS-5), (c) 20 wt % (TS-20), and (d) 80 wt % (TS-80) TiO_2, respectively.

Ti/Si binary oxides having a low Ti content (TS-1, TS-5) exhibit an intense single pre-edge peak, indicating that the titanium oxide species have a tetrahedral coordination in the SiO_2 matrixes. The tetrahedrally Ti such as $Ti(OPr^i)_4$ are known to exhibit an intense single pre-edge peak due to the lack of an inversion center in the regular tetrahedron structure. As can be seen in Figure 2-9, for the Ti/Si binary oxide having a high Ti content of 20 wt % TiO_2 (TS-20), the single characteristic pre-edge peak is rather weak, indicating that the catalyst consists of a mixture of tetrahedrally and octahedrally coordinated titanium oxide species. On the other hand, the Ti/Si binary oxide having a large Ti content of 80% as TiO_2 (TS-80) exhibits three characteristic weak preedge peaks. Because these characteristic small pre-edge peaks can be attributed to the transitions from the core level of Ti to three different kinds of molecular orbitals ($1t_{1g}$, $2t_{2g}$ and $3e_g$) of anatase TiO_2, these observation indicate the presence of the crystalline anatase TiO_2, being in good agreement with the results XRD analysis.

Figure 2-9 also shows the Fourier transforms of EXAFS spectra (FT-EXAFS) of the catalysts, and all data are given without corrections for phase shifts. All of the catalysts investigated in the present study exhibit a strong peak at around 1.6 Å which can be assigned to the neighboring oxygen atoms (Ti-O). The Ti/Si binary oxides having low Ti contents of 1 and 5 wt% TiO_2 (TS-1, TS-5) exhibit only Ti-O peaks, indicating the presence of the isolated titanium oxide species on these catalysts. From the results by the curve-fitting analysis (R factor of the accuracy of the curve fitting: 9.0%) of the EXAFS spectra, as can be seen in Figure 9, it was

found that the Ti/Si binary oxide having the lowest Ti content (TS-1) consists of 4-coordinate titanium ions with a coordination number (N) of 4.1 ± 0.5 and an atomic distance (R) of 1.82 ± 0.02 Å. This atomic distance is similar to those observed with tetrahedrally coordinated titanium oxide which is anchored onto Vycor glass by the CVD method [13]. It should be mentioned that atomic distance of the Ti-O bond of the highly dispersed tetrahedrally coordinated titanium oxide species is shorter by 0.14 Å than that of the bulk TiO_2 of 1.96 Å [14].

As shown in Figure 2-9, the Ti/Si binary oxide having a large Ti content (TS-80) exhibits an intense peak at around 2.7 Å. This peak can be assigned to the neighboring titanium atoms behind the oxygen (Ti-O-Ti), indicating the aggregation of the titanium oxide species in these catalysts [14, 15]. Results of the coordination number (N) of 5.9±0.5 and atomic distance (R) of 1.91±0.02 Å for the Ti/Si binary oxide having a large Ti content (TS-80) obtained by curve-fitting analysis (R factor of the accuracy of the curve fitting: 8.2%) of the EXAFS spectra suggest the presence of an aggregated octahedral titanium oxide species with this catalyst.

These XANES and FT-EXAFS investigations indicate that the Ti/Si binary oxides having a low Ti content involve only the well-isolated tetrahedral titanium oxide species whose local structure is maintained in the regions having the Ti content of less than 20 wt % TiO_2, while the Ti/Si binary oxides having a large Ti content involve the aggregated octahedral titanium oxide species (anatase TiO_2 phase).

To investigate the local structure of the titanium oxide species in

Ti/Si binary oxide catalysts, an ESR technique was incorporated to monitor the Ti^{3+} ions which were formed by the photoreduction of the oxide with H_2 at 77 K (1), maintaining the coordination geometry of the original Ti^{4+} species [14, 32].

$$(Ti^{4+}-O^{2-})+H_2 \rightarrow (Ti^{3+}-OH^{-})+H \qquad (1)$$

As shown in figure 2-10, the ESR spectrum of Ti^{3+} ions formed in this way in the Ti/Si binary oxide having a low Ti content of 5 wt % TiO_2 (TS-5) shows two different types of Ti^{3+} signals with g value of $g_{\perp}$=1.981 and 1.962. The addition of H_2O onto the sample led to a decrease in the intensity of the ESR signal with a value of $g_{\perp}$=1.981, the extent depending on the amount of H_2O added. Furthermore, the addition of excess amount of H_2O led to a complete disappearance of the signal. Simultaneously, the addition of H_2O also led to an increase in the intensity of the ESR signal with a value of $g_{\perp}$=1.962. From the g value of $g_{\perp}$=1.981 and the characteristic shape of the spectrum as well as the spectrum changes by the addition of H_2O, it can be concluded that the Ti^{3+} species are present in a tetrahedral coordination and that the original Ti^{4+} oxide species were also present in a tetrahedral coordination, since the photoreduction of the oxide at 77 K did not modify the coordination structure of the Ti^{4+} ions [14,32]. The ESR signal with a *g* value of 1.962 can be assigned as the coordinatively saturated Ti^{3+} species having H_2O or OH^- as ligands. These H_2O or OH^- species are formed by the processes of the photoreduction of Ti^{4+} ions by H_2

at 77 K. On the other hand, the Ti/Si binary oxide having a large Ti content (TS-80) exhibits an intense and sharp ESR signal with a value of $g_{\perp}$ =1.990. This characteristic ESR signal indicates the presence of the aggregated octahedral titanium oxide species [32].

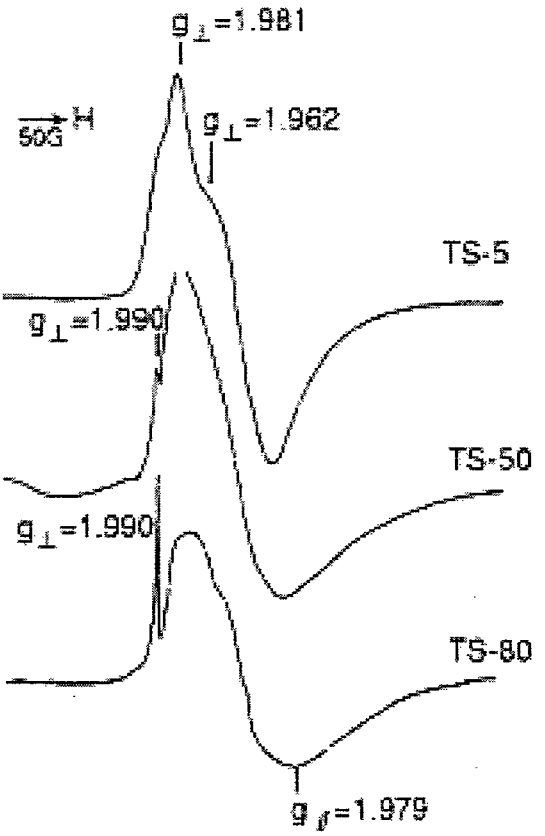

Figure 2-10. ESR spectra of the Ti^{3+} ions generated by the photoreduction of Ti/Si binary oxides with H_2 at 77 K. ESR signal was also recorded at 77 K. TS-5, TS-50, and TS-80 samples are the Ti/Si binary oxides of 5, 50, and 80 wt % TiO_2, respectively.

UV irradiation of the Ti/Si binary oxides in the 1-octanol-acetonitrile solution in the presence of O_2 led to the photocatalytic oxidation of 1-octanol to 1-octanal as the major reaction. The selectivity for the formation of 1-octanal at the initial stage of the reaction was >95% on the binary oxides having Ti content lower than 20 wt % TiO_2. No products could be detected in the dark under the same reaction conditions. Figure 8 shows the specific photocatalytic reactivities of the catalysts per unit weight of TiO_2. A remarkable increase in the specific photocatalytic reactivity of the catalysts can be seen for the catalysts having a low Ti content while a slight increase can be seen for the catalysts having a high Ti content. The specific photocatalytic reactivity of these binary oxides having Ti content of 0.4 - 5 wt % TiO_2 was found to be much higher than that of the "standard TiO_2 catalyst", anatase TiO_2 (Degussa P-25). The quantum yield determined with the binary oxide at 1 wt % TiO_2 under the UV irradiation (λ=300nm) of light flux of 1×10^{17}/min cm^3 was 22 %, while it was 12 % for TiO_2 (P-25) and 4 % for TiO_2 powder by the same sol-gel method. These findings indicate that Ti/Si binary oxides, especially the oxides having a low Ti content prepared by the sol-gel method, are promising photocatalysts to be used in liquid-phase reactions.

As shown in Fig. 2-11, the addition of H_2O or CH_3CCH molecules onto the Ti/Si binary oxides leads to an efficient quenching of the photoluminescence and shortening of its lifetime, their extent depending on the amount of added gasses. Such an efficient quenching of the photoluminescence with H_2O or CH_3CCH indicates that added CH_3CCH or

H_2O interacts and/or reacts with the titanium oxide species in the excited state.

UV irradiation of the Ti/Si binary oxides in a gaseous mixture of CH_3CCH and H_2O led to the hydrogenolysis reaction accompanied by a C≡C bond fission to produce CH_4 and C_2H_6 as well as hydrogenation without the C≡C bond fission to from C_3H_6 as the main products.

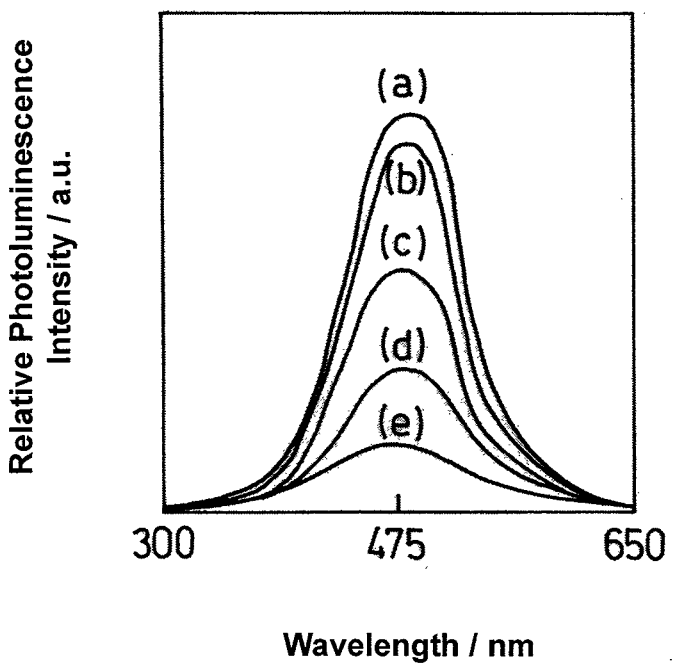

Figure 2-11. Photoluminescence spectra of the Ti/Si binary oxide (TS-5) (a), and the effects of the addition of CH_3CCH and H_2O (b-e) on the photoluminescence spectrum. Measured at 77 K, excitation at 290 nm, pressure of added CH_3CCH: (b) 2, (d) 20 Torr, and H_2O: (c) 0.5, (e) 10 Torr.

As shown in Fig. 2-12, the hydrogenolysis reaction (C_2H_6 formation) is predominant in regions of low Ti content, while the hydrogenation reaction (C_3H_6 formation) also proceeds efficiently in regions of high Ti content. As described previous literature [2], the hydrogenolysis reaction is attributed to the close existence of the photoformed electron and hole, i.e., Ti^{3+} - O^- pair species. The charge transfer excited state of the isolated tetrahedral titanium oxide species formed in the Ti/Si binary oxides having low Ti content plays a significant role as the reactive species which lead the efficient hydrogenolysis reaction. On the other hand, the Ti/Si binary oxides having high Ti content contain the aggregated TiO_2 fine particle on which the photocatalytic reaction in the same manner as on bulk TiO_2 catalysts become predominant and the reduction reaction by electrons and the oxidation reaction by holes occur separately from each other on different sites, leading to the selective formation of C_3H_6 (hydrogenation reaction).

In Fig. 2-12, an increase in photocatalytic activity of the titanium oxide species in regions of low Ti content as well as increase in regions of high Ti content can be observed. The specific photocatalytic activity of the titanium oxide species (normalized by unit weight of the titanium oxide) in the binary oxides with low Ti content was found to be higher than that of the Degussa P-25 anatase TiO_2. These findngs indicate that the Ti/Si binary oxides prepared by the sol-gel method are useful and promising as a photocatalyst. Furthermore, in regions of low Ti content, there was a good parallel between the photocatalytic activity of the titanium oxide species and the yield of the photoluminescence of the Ti/Si binary oxides, suggesting

that the appearance of such high photocatalytic activity is closely associated to the formation of the charge transfer excited complex, i.e., the Ti^{3+} - O^- pair, of the highly dispersed tetrahedral titanium oxide species.

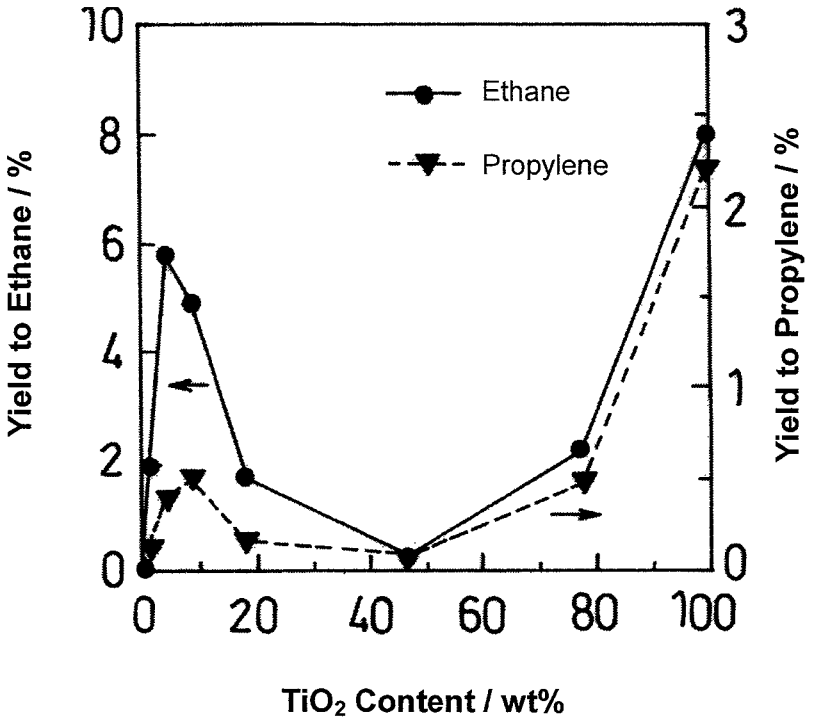

Figure 2-12. The effects of Ti content on the photocatalytic activities of Ti/Si binary oxides for the hydrogenation (C_3H_6 formation) and hydrogenolysis (C_2H_6 formation) of CH_3CCH with H_2O. The yields obtained after photoreaction for 2 h.

The effect of Pt-loading on the photocatalytic reactivity of Ti/Si binary oxides has also been investigated. Although the addition of Pt onto the Ti/Si binary oxides is effective in an increase in the photocatalytic reactivity, only the formation of C_3H_6 (hydrogenation reaction) is promoted, accompanied by a decrease in the formation of C_2H_6 (hydrogenolysis

reaction) independently of the Ti content of binary oxides.

Pt-loading onto the Ti/Si binary oxide having a low Ti content led to an efficient quenching of the photoluminescence, accompanied by the shortening of its lifetime. Because the results obtained by EXAFS and absorption measurements indicated that the local structure of the Ti/Si binary oxide having a low Ti content was not altered by the Pt-loading, the effective quenching of the photoluminescence can be attributed to the electron transfer from the photo-excited titanium oxide species to Pt metals. As a result, on the Pt-loaded the Ti/Si binary oxide having a low Ti content, photocatalytic reactions which proceed in the same manner as on bulk TiO_2 become predominant, meaning that the reduction reaction by electrons and the oxidation by holes occurring separately from each other on different sites become predominant, leading to the selective formation of C_3H_6 (hydrogenation reaction).

As described above, in situ photoluminescence, UV-vis reflectance, FT-IR, ESR, XAFS, XRD, and XPS spectroscopic investigations of these Ti/Si binary oxides indicated that the titanium oxide species are highly dispersed in the SiO_2 matrixes and exist in a tetrahedral coordination. Such titanium oxide species exhibited the distinct and characteristic photoluminescence, and its yield increased when the Ti content in the Ti/Si binary oxides was decreased. As shown in Figure 8, a parallel relationship between the specific photocatalytic reactivities of the titanium oxide species and the yield of the photoluminescence of the Ti/Si binary oxide catalysts can clearly be seen. It is clear that the high photocatalytic reactivity of the

Ti/Si binary oxide is closely associated with the formation of the charge-transfer excited complexes of the highly dispersed tetrahedral titanium oxide species and their high reactivities.

On the other hand, such photocatalytic reactivity could not be observed for Ti/Si binary oxides in the middle region of Ti content of about 50 wt % TiO_2. XPS and XRD investigations of the catalysts suggested that the segregation of SiO_2 in the surface regions of the binary oxides is remarkable for the catalyst having a Ti content of about 50 wt % TiO_2. The covering of the titanium oxide species with such SiO_2 moieties suppresses and disturbs the accessibility of the reactant molecules with the active site of the titanium oxide species, resulting in a dramatic decrease in the photocatalytic reactivity of the catalysts.

2. 4 Conclusions

Ti/Si binary oxides having different Ti content were prepared using the sol-gel method and used as photocatalysts. When the Ti content is decreased, the crystalline structure of the titanium oxide changes from aggregates in an anatase phase to ultrafine species in an amorphous state. In Ti/Si binary oxides having lower Ti content, the isolated titanium oxide species in tetrahedral coordination were present separately from each other in the SiO_2 matrixes and exhibited a characteristic photoluminescence spectrum attributed to the radiative decay from the charge-transfer excited state of these species.

The excited state of these tetrahedrally coordinated titanium oxide species plays a significant role in the liquid-phase photocatalytic oxidation of 1-octanol to 1-octanal as an active site, their roles being similar to the photocatalysis in the gas phase.

In the photocatalytic hydrogenolysis reaction (C_2H_6 formation), the good parallel between the yield of the photoluminescence and the yield of the photocatalytic reaction obtained clearly indicated that the charge transfer excited state of titanium oxide species in a tetrahedral coordination plays a significant role in the photocatalytic reaction, especially for the hydrogenolysis reaction.

The present study clearly demonstrates that Ti/Si binary oxides by the sol-gel method are promising candidates as new and efficient photocatalysts and the control of the charge separation is important in developing highly efficient and selective photocatalysts.

2. 5 References

[1] Photocatalytic Purification and Treatment; D. F. Ollis and H. Al-Ekabi, Eds.; Elsevier: Amsterdam (1993).

[2] M. Anpo, *Res. Chem. Intermed.*, 9, 67 (1989), M. Anpo, *Catal. Surv. Jpn.*, 1, 169 (1997).

[3] M. Anpo and H. Yamashita, in Surface Photochemistry, M. Anpo, Ed.; Wiley, West Sussex, 117 (1996).

[4] Photocatalysis: Fundamentals and Applications; N. Serpone, and E. Pelizzetti, Eds.; John Wiley & Sons: New York (1989).

[5] M. A. Fox and M. T. Dulay, *Chem. Rev.*, 93, 341 (1993).

[6] P. V. Kamat, *Chem. Rev.*, 93, 267 (1993).

[7] M. R. Hoffmann, S. T. Martin, W. Choi, D. W. Bahnemann, *Chem. Rev.*, 95, 69 (1995).

[8] A. L. Linsebigler, G. Lu, J. T. Yates, *Chem. Rev.*, 95, 735 (1995).

[9] K. I. Zamaraev, M. I. Khramov, V. M. Parmon, *Catal. Rev. –Sci. Eng.*, 36, 617 (1994).

[10] A. Heller, *Acc. Chem. Res.*, 28, 503 (1995).

[11] M. Anpo, N. Aikawa, Y. Kubokawa, M. Che, C. Louis, E. Giamello, *J. Phys. Chem. Rev.*, 89, 5017, 5689 (1985).

[12] M. Anpo, and K. Chiba, *J. Mol. Catal.*, 74, 207 (1992).

[13] H. Yamashita, Y. Ichihashi, M. Harada, G. Stewart, M. A. Fox, M. Anpo, *J. Catal.*, 158, 97 (1996).

[14] H. Yamashita, Y. Ichihashi, M. Anpo, M. Hashimoto, C. Louis, M. Che, *J. Phys. Chem.*, 100, 16041 (1996).

[15] M. Anpo, H. Yamashita, Y. Ichihashi, Y. Fujii, M. Honda, *J. Phys. Chem. B.*, 101, 2632 (1997).

[16] H. Yamashita, Y. Ichihashi, S. G. Zhang, Y. Matsumura, Y. Souma, T. Tatsumi, M. Anpo, *Appl. Surf. Sci.*, 121&122, 305 (1997).

[17] D. Avnir, *Acc. Chem. Res.*, 28, 328 (1995).

[18] N. Negishi, M. Matsuoka, H. Yamashita, M. Anpo, *J. Phys. Chem.*, 97, 5211 (1993).

[19] S. C. Moon, M. Fujino, H. Yamashita, M. Anpo, *J. Phys. Chem. B.*, 101, 369 (1997).

[20] M. Anpo, N. Nakayama, S. Kodama, Y. Kubokawa, K. Domen, T. Onishi, *J. Phys. Chem.*, 90, 1633 (1985).

[21] S. Imamura, T. Nakai, H. Kanai, T. Ito, *J. Chem. Soc., Faraday Trans.* 91, 1261 (1995).

[22] Z. Liu and R. J. Davis, *J. Phys. Chem.*, 98, 1253 (1994).

[23] R. J. Davis and Z. Liu, *Chem. Mater.*, 9, 2311 (1997).

[24] H. Yamashita, M. Matsuoka, K. Tsuji, Y. Shioya, M. Anpo., *J. Phys. Chem.*, 100, 397 (1996).

[25] M. A. Camblor, A. Corma, J. Prez-Pariente, *J. Chem. Soc. Chem. Commun.*, 557 (1993).

[26] A. Y. Stakheev, E. S. Shpiro, J. Apijok, *J. Phys. Chem.*, 97, 5668 (1993).

[27] M. Anpo, T. Kawamura, S. Kodama, *J. Phys. Chem.*, 92, 438 (1988).

[28] S. Bordiga, S. Coluccia, C. Lamberti, L. Marchese, A. Zecchina, F. Boscherini, F. Buffa, F. Genoni, G. Leofanti, G. Petrini, G. Vlaic, *J. Phys. Chem.*, 98, 1253 (1994).

[29] L. Bonneviot, D. T. On, A. Lopez, *J. Chem. Soc., Chem. Commun.* 685 (1993).

[30] T. Maschmeyer, F. Rey, G. Sankar, J. M. Thomas, *Nature*, 378, 159 (1995).

[31] S. Yoshida, T. Takenaka, T. Tanaka, H. Hirano, H. Hayashi, *Stud. Surf. Sci. Catal.*, 101, 871 (1996).

[32] M. Anpo, T. Shima, T. Fujii, S. Suzuki, M. Che, *Chem. Lett.*, 1997 (1987).

Chapter 3

Photocatalytic Synthesis of CH_4 and CH_3OH from CO_2 and H_2O on Highly Dispersed Titanium Oxide Species

3. 1 Introduction

The photosynthetic reduction of CO_2 with H_2O is of vital interest especially as one of the most desirable goals for the utilization of solar energy [1]. Since the efficiency of the photosynthetic reduction of CO_2 on catalytic surfaces is still quite low, great efforts must be made to understand the fundamental reaction mechanisms in order to improve the efficiency [2,3]. With well-defined highly dispersed catalysts, it is possible not only to achieve more active and selective photocatalytic system but also to obtain detailed information on the nature of active sites and the reaction mechanism at the molecular level [4,5].

In the present work, the photocatalytic reduction of CO_2 with H_2O to produce CH_4, CH_3OH, and CO on highly dispersed titanium oxide anchored onto transparent porous Vycor glass (PVG) and zeolites by an anchoring or ion-exchange method and incorporated into Ti/Si binary oxides prepared by the sol-gel method has been investigated by means of in situ photoluminescence, ESR, UV and XAFS measurements and an analysis of the photoreaction products.

3. 2 Experimental

Anchoring was performed using a facile reaction between the titanium compound with the surface OH groups of PVC(Corning code 7930) and zeolite (ZSM-5: Si/Ai=23.3, surface area 256 m^2/g; Y-zeolite: Si/Ai=5.5,

710 m^2/g) in the gas phase at 473K, followed by treatment with H_2O vapor to hydrolyze the anchored compounds. Ion-exchange with an aqueous solution of $TiCl_3$ was also carried out. Ti-Si binary oxides with differing TiO_2 contents were prepared by the sol-gel method using mixtures of tetraethylorthosilicate (TEOS) and titanium-isopropoxide (TPOT). Thus formed highly dispersed samples were washed and finally calcined in air at 773 K.

UV irradiation was carried out using a 75 W high-pressure Hg lamp through water and color filters (λ>280 nm) at 273-323 K. ESR spectra with X-bands and the photoluminescence spectra were recorded at 77 K. The UV absorption spectra and Ti K-edge XAFS spectra (XANES and EXAFS) in the fluorescence mode were recorded at 295 K. The photoreaction products were analyzed by gas chromatography and mass spectrometry.

3. 3 Results and Discussion

Significant blue shifts of the UV absorption bands were observed for titanium oxides anchored on PVC and zeolite when compared with TiO_2 bulk powder. This blue shifts can be explained in terms of the quantum size effect. The significant blue shift indicates the presence of highly dispersed titanium oxide species on the supports.

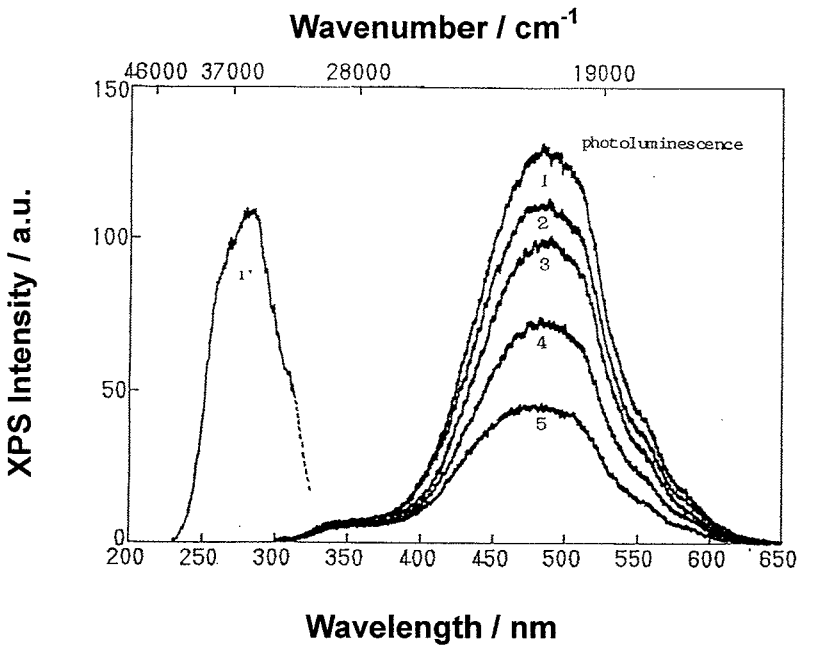

Figure 3-1. Photoluminescence spectrum of the anchored titanium oxide on PVG at 77 K (1), its excitation spectrum (1'), and the quenching by added H_2O (2-4) and CO_2 (5). Excitation beam; 280 nm, emission monitored at 480 nm, amounts of added H_2O: 1) 0.0, 2) 42.6, 3) 77.4, 4) 204 μ molg^{-1}; amounts of added CO_2: 5) 25.6 μ molg^{-1}.

Figure 3-1 (1) shows a typical photoluminescence spectrum of the titanium oxide anchored onto PVC(1) and its excitation spectrum at 77 K (1'). The excitation with light brought about an electron transfer from oxygen to titanium ion, resulting in the formation of trapped pairs of a hole center (O^-) and an electron center (Ti^{3+}) [5]. In this way, the absorption and photoluminescence spectra are attributed to the charge transfer processes on the anchored titanium oxide species on the support surface. As shown in fig. 3-1 (2-5), the addition of H_2O or CO_2 molecules at 275 K onto the anchored titanium oxide leads to an efficient quenching of

the photoluminescence with different efficiencies. Such an efficient quenching of the photoluminescence with CO_2 or H_2O suggests not only that the emitting sites are highly dispersed on the surfaces, but also that added CO_2 or H_2O interacts and/or reacts with the anchored titanium oxide species in both its ground and excited states.

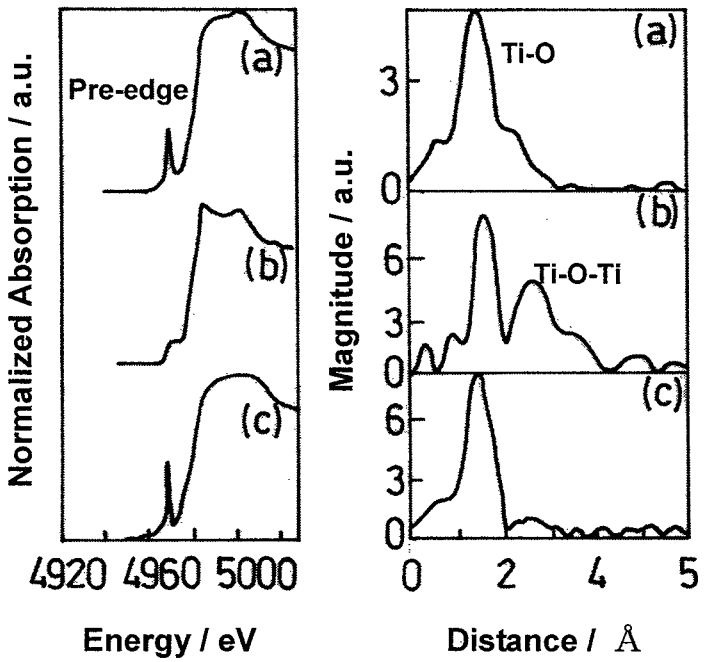

Figure 3-2. Ti K-edge XANES spectra (left) and FT-EXAFS spectra (right) of (a) the titanium oxide anchored on PVG, (b) a bulk TiO_2 (anatase), and (c) TPOT.

Figure 3-2 shows the XANES ant FT-EXAFS spectra of the titanium oxide anchored on PVC, a bulk TiO_2 (anatase) and TPOT. Although the bulk TiO_2 exhibits three small pre-edge peaks, the titanium oxide anchored on PVC exhibits only a single and pre-edge peak which is similar to that of

TPOT, indicating the presence of tetrahedrally coordinated titanium oxide species on the surface [6]. The FT-EXAFS spectra of the titanium oxide anchored on PVG (fig. 2-a) exhibits only a Ti-O peak, indicating the presence of an isolated titanium oxide species. These results obtained by UV, photoluminescence, and XAFS measurements indicate that highly dispersed isolated tetrahedral titanium oxide species were formed on PVG and zeolites by the anchoring method.

UV irradiation of the anchored titanium oxide Catalysts in the presence of a mixture of CO_2 and H_2O led to the evolution of CH_4, CH_3OH, and CO in the gas phase at 323 K, as well as trace amounts of C_2H_4 and C_2H_6. However, no product could be detected in the dark conditions.

Figure 3-3 shows the time profiles for the production of CH_4 and CO with the UV irradiation time. The yields of these products are in a good linear relationship with the irradiation time. The total yields of CH_4, CH_3OH, and CO were larger under UV-irradiation at 323 K than those at 275 K. It is clear that the photocatalytic reactions at higher temperatures proceed efficiently and more catalytically.

Figure 3-3 also shows the effect of the H_2O/CO_2 ratio on the photocatalytic activity. As shown in Fig. 3, the efficiency of the photocatalytic reaction strongly depends on the ratio of the H_2O/CO_2 and the activity increases with an increase of the H_2O/CO_2 ratio; however, an excess amount of H_2O suppresses the reaction rates. It was found that optimum ratio of H_2O/CO_2 strongly depends on the type of supports.

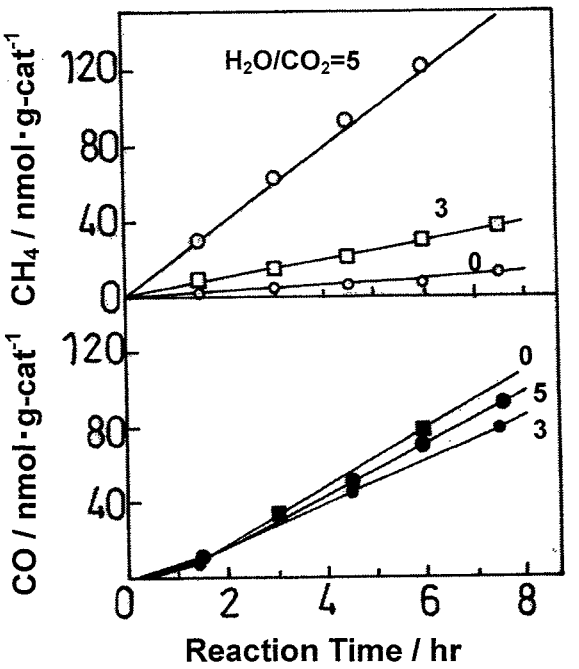

Figure 3-3. The time profiles of the photoreaction of CO_2 and H_2O to produce CH_4 and CO on the titanium oxide anchored on PVG and the effect of the H_2O/CO_2 ratio on the yields of these products. Numbers represent the ratio of H_2O/CO_2.

Figure 3-4 shows the effect of the support on the distribution (selectivity) and yields of the photoproducts on the anchored titanium oxide catalysts. There is a remarkable difference in the reactivity and selectivity among the catalysts. The CO is formed as a main product on the titanium oxide anchored on ZSM-5, whereas the titanium oxide anchored on Y-zeolite and PVC exhibited the highest photocatalytic activity and the highest selectivity for the formation of CH_4 and CH_3OH.

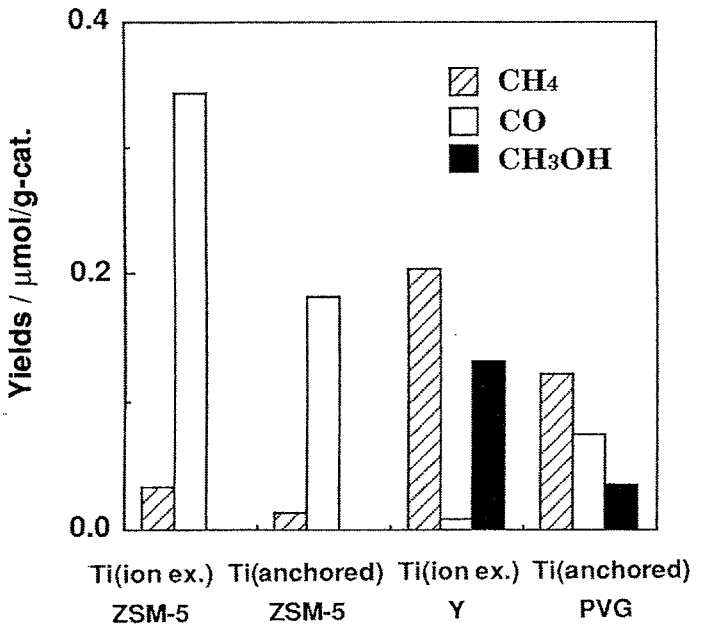

Figure 3-4. The effect of the support on the distribution and yields of the photo-products.

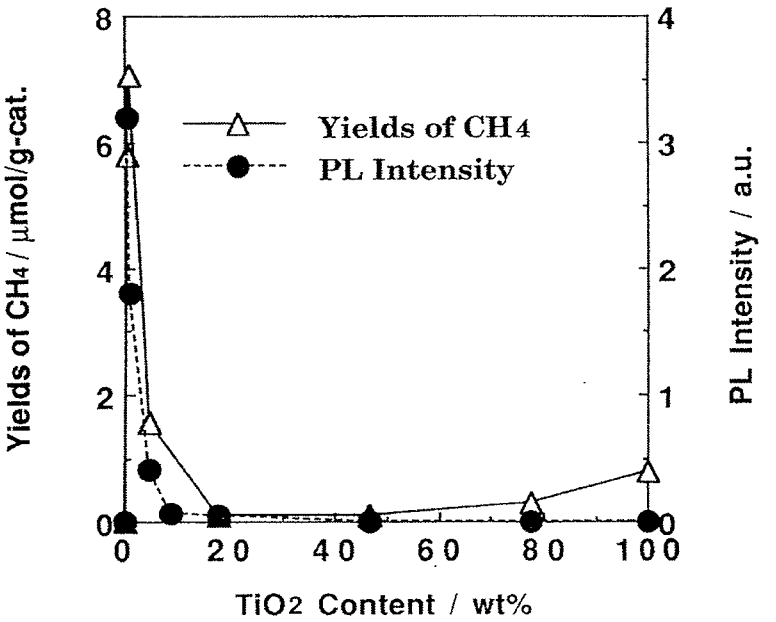

Figure 3-5. The effects of the TiO_2 contents on the yields of CH_4 and the relative intensity of photoluminescence (at 77 K) of the Ti-Si binary oxide catalyst.

Figure 3-5 showed the effect of the TiO_2-contents on the yields of the photoluminescence attributed to the presence of tetrahedral coordinated titanium oxide species at 77 K and the yields of the photocatalytic reduction of CO_2 with H_2O on the Ti/Si binary oxide catalysts prepared by the sol-gel method. XAFS, ESR and photoluminescence investigation of these Ti/Si binary oxide catalysts showed that the tetrahedral coordination is sustained in these catalysts until the TiO_2-content reaches to about 10 wt%. Thus, it is clear that the Ti/Si binary oxide catalysts with TiO_2-contents up to about 10 wt% are successfully designed as the active photocatalyst for the reduction of CO_2 with H_2O at 323 K.

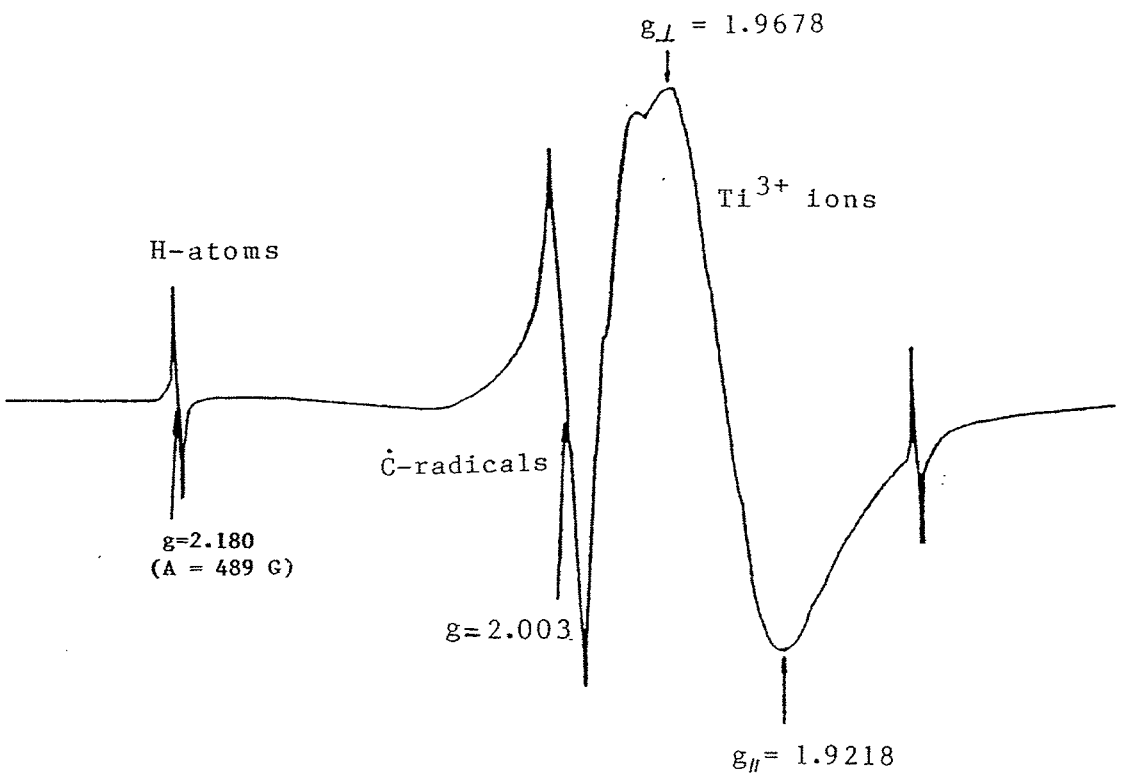

Figure 3-6. ESR signals at 77 K of the titanium oxide anchored on PVG after the irradiation in the presence of CO_2 (7 μ molg^{-1}) and H_2O (μ molg^{-1}).

UV-irradiation of the anchored titanium oxide catalyst in the presence of CO_2 and H_2O at 77 K led to the appearance of ESR signals due to Ti^{3+}ions, H atoms and C radicals as shown in Fig. 3-6. These ESR signals increased in intensity with UV-irradiation time at 77 K and found to disappear once the temperature of the cell was raised to 275 K. In this system the formation of CH_4 was detected as a product. The relative intensities of these ESR signals strongly depended on the amount of CO_2 and H_2O on the catalyst, the intensity of the H atoms increasing with increasing the amount of H_2O, while the intensity of the Ti^{3+}ions decreased.

As shown in Fig. 3-7, the addition of H_2O or CO_2 molecules onto the Ti/Si binary oxides leads to an efficient quenching of the photoluminescence and shortening of its lifetime, their extent depending on the amount of added gasses. Such an efficient quenching of the photoluminescence with CO_2 or H_2O indicates that added CO_2 or H_2O indicates that added CO_2 or H_2O interacts and/or react with the titanium oxide species in the excited state. For the quenching of the photoluminescence in its intensity and lifetime, CO_2 is less effective than H_2O, indicating that the interaction of CO_2 with the charge transfer excited state of the titanium oxide species is weaker than H_2O.

From these results, the reaction mechanism in the photocatalytic reduction of CO_2 with H_2O on the highly dispersed titanium oxide catalyst can be proposed. CO_2 and molecules interact with the excited state of photoinduced $(Ti^3 + \cdot O^-)^*$ species and the reduction of CO_2 and the decomposition of H_2O proceed competitively. Furthermore, H atoms and

OH radicals are formed from H_2O and these radicals react with the carbon species formed from CO_2 to produce CH_4 and CH_3OH. The amounts of the absorbed reactant and of the desorbed products strongly depend on the nature of the supports.

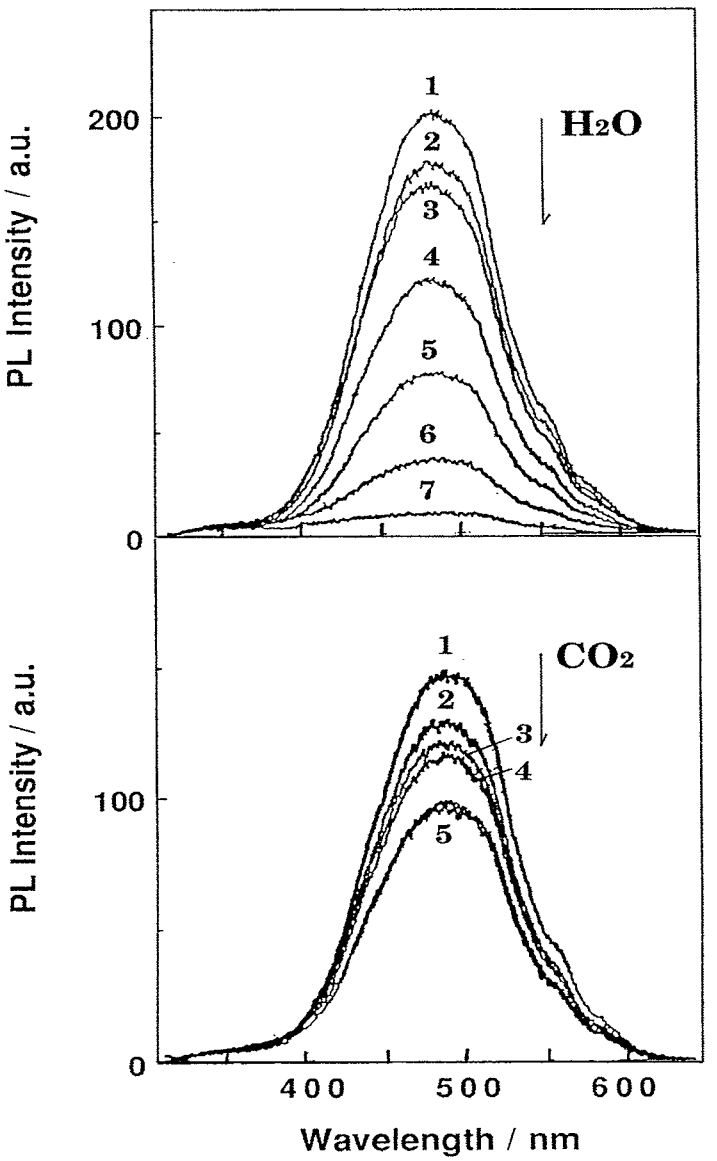

Figure 3-7. Photoluminescence spectrum (a) of the Ti/Si binary oxide (5 wt %) as TiO_2 upon excitation at 280 nm at 77 K and the effects of addition of gasses. (A) H_2O: 3) 0.1, 4) 0.5, 5) 1.0, 6) 5.0, 7) 10; (B) CO_2: 2) 0.5, 3) 1.0, 4) 5.0, 5) 10 Torr.

3. 4 Conclusions

The photosynthetic reduction of CO_2 with H_2O produce CH_4, CH_3OH, and CO has been found to proceed on highly dispersed titanium oxides anchored onto PVC and zeolites and incorporated in Ti-Si binary oxides. Highly dispersed isolated tetrahedral titanium oxide species were considered to be the active sites for reaction system. The product distribution was found to strongly depend on the type and chemical nature of the supports.

3. 5 References

[1] M. Anpo and K. Chiba, *J. Mol. Catal.*, 74, 207 (1992).

[2] H. Yamashita, S. Ehara, M. Anpo, *Res. Chem. Intermedi.*, 20, 815 (1994).

[3] H. Yamashita, H. He, K. Tanaka, M. Anpo, *Chem. Lett.*, 855 (1994).

[4] M. Anpo, M. Matsuoka, H. Yamashita, *J. Phys. Chem.*, 98, 5744 (1994).

[5] M. Anpo, *Res. Chem. Intermedi.*, 11, 67 (1989).

[6] H. Yamashita, S. Kawasaki, M. Anpo, *Shokubai.*, 36, 440 (1994).

Chapter 4

Efficient Adsorption and Photocatalytic Degradation of Organic Pollutants Diluted in Water Using the Fluoride-Modified Hydrophobic Titanium Oxide Photocatalysts: Ti-containing Beta zeolite and TiO_2 loaded on HMS mesoporous silica

4. 1 Introduction

The design of highly efficient and selective photocatalytic systems is of vital interest. It has been found that the highly dispersed titanium oxide photocatalysts anchored on the porous silica-based materials exhibit high and characteristic photocatalytic reactivity compared to bulk TiO_2 powder. Especially the titanium oxide species prepared within the pores and frameworks of zeolite and mesoporous silica have been revealed to have unique local structures as well as high reactivities in the various photocatalytic reactions in the gas phase [1].

Recently a large-pore Ti-containing zeolite, Ti-Beta, has been hydrothermally synthesized by various methods. Davis et al. have prepared aluminum-free Ti-Beta zeolite using N'-dibenzyl-4,4'-trimethylenebis (N-methylpiperidinium) dihydroxide as a structure-directing agent (SDA) in the absence of seeding [2] and found that the calcined sample exhibits the high H_2O affinity. On the other hand, Corma et al. has reported that aluminum-free Ti-Beta zeolite can be prepared in the F^- medium and performs as a hydrophobically selective oxidation catalyst [3]. The H_2O affinity of Ti-Beta zeolites changes significantly depending on the preparation methods and their hydrophobic-hydrophilic properties can modify not only the catalytic properties but also the photochemical process in the zeolite pores [4]. On the other hands, various types of mesoporous silica have been synthesized and been found to be useful as the supports of TiO_2 photocatalyst.

Generally, these mesoporous silica has the hydrophilic surface property and this hydrophilic surface often affects to the photocatalytic reactions.

The photocatalytic degradation of organic toxic compounds dissolved in aqueous solutions at low concentrations using irradiated titanium oxide is one of the most promising applications of photocatalysts [5-10]. It is effective to use the hybrid materials, combined with adsorbents and photocatalysts for the purification of water. Zeolite and mesoporous silica which have high surface area and porous structure, have been used as conventional adsorbents. The condensation properties of these adsorbents should depend on their surface hydrophilic-hydrophobic properties and the highly hydrophobic surface seems to be suitable for the adsorption of organic compounds diluted in water. The fine titanium oxide photocatalyst loaded on hydrophobic zeolite and mesoporous silica have opened new possibilities for photocatalytic degradation of various organic compounds diluted water.

In the present study, we have used the two types of Ti-Beta zeolites synthesized under different conditions as photocatalysts for the liquid phase degradation of organic compounds (2-propanol) diluted in water to form CO_2 with H_2O and the effects of the hydrophobic-hydrophilic properties of zeolites on the photocatalytic reactivity have been investigated. Furthermore, the TiO_2 photocatalysts loaded on the fluoride-modified hydrophobic mesoporous silica were prepared. Using these hydrophobic supports and photocatalysts, the adsorption properties and photocatalytic reactivities for the degradation of 2-propanol diluted in water have been studied.

4. 2 Experimental

4. 2. 1 Catalysts

Ti-Beta zeolites (Si/Ti=60) were synthesized using two kinds of SDA: N'-dibenzyl-4,4'-trimethylenebis(N-methylpiperidinium) dihydroxide and tetraethylammonium fluoride (TEAF) [2,3]. The sources of the silica and titanium oxide were tetraethylorthosilicate and titaniumisopropoxide, respectively. The two types of Ti-Beta zeolites are denoted according to the kinds of SDA, i.e., Ti-Beta(OH) and Ti-Beta(F). The material mixture for Ti-Beta(OH) had the following composition: 1 SiO_2/ 0.02 TiO_2/ 0.2 N'-dibenzyl-4,4'-trimethylenebis (N-methylpiperidinium) dihydroxide / 30 H_2O in molar ratio. The material mixture for Ti-Beta(F) had the following composition: 1 SiO_2/ 0.02 TiO_2/ 0.56 TEAF/ 7 H_2O. The gelation of the material mixtures were carried out at room temperature, and these gel mixtures were placed into Teflon-lined stainless autoclaves and heated at 413 K for 5 days while being rotated at 60 rpm. The product was collected by centrifugal filtration, washed with distilled water, and dried in air at 353 K. To remove the occluded organic molecules, the samples were heated under a flow of dry air at 823 K for 4 h. TS-1 (Si/Ti=60, MFI) was prepared from a material mixture having the following composition: 1 SiO_2 / 0.02 TiO_2 / 0.4 tetrapropylammonium hydroxide (TPAOH) / 30 H_2O.

TiO_2 powdered catalysts (Degussa, P-25: anatase 92 %, rutile 8 %) were supplied as standard reference.

The synthesis of the hydrophobic mesoporous silica (denoted as HMS(F)) was performed using tetraethyl orthosilicate (TEOS), tetraethylammonium fluoride (TEAF) as the source of the fluoride and dodecylamine (DDA) [11]. TEOS dissolved in a mixture of 2-propanol and ethanol and DDA (0~7.75g) dissolved in water with HCl (3ml) are mixed, following to stirring at 295 K for 24 h. The precursor mixture was washed by distilled water, dried at 373 K for 24 h, and then calcined at 823 K for 7 h. The ratio of TEAF to DDA was 0 (HMS), 0.25 (HMS(F1)), 0.75 (HMS(F2)) and 1.25 (HMS(F3)). Furthermore, imp-TiO_2/HMS(F) (10 wt% as TiO_2) was prepared by impregnating HMS(F) with an aqueous titanium oxalate solution, then dried and calcined for 5 h at 773 K.

4. 2. 2 Photocatalytic reaction

4. 2. 2. 1 Liquid-phase degradation

The photocatalytic reactions were carried out with the catalysts (50mg) in the quartz tube with a 2-propanol aqueous solution ($2.6x10^{-3}$ M, 25 ml). The sample was irradiated at 295 K using UV light ($\lambda > 280$nm) from a 100W high-pressure Hg lamp with stirring under O_2 atmosphere in the system [10]. The reaction products were analyzed by gas chromatography. The photocatalytic reactivity was estimated from the initial decrease in the concentration of 2-propanol after preadsorption of 2-propanol on the catalyst under dark condition for 60 min.

4. 2. 2. 2 Gas-phase reactions

Reduction of CO_2 with H_2O and NO decomposition were performed. Prior to the photoreactions and spectroscopic measurements, the catalysts were degassed at 725 K for 2 h, heated in O_2 at the same temperature for 2 h and finally evacuated at 475 K to 10^{-6} Torr for 1 h.

The photocatalytic reduction of CO_2 with H_2O was carried out with the catalysts (50 mg of the catalyst involving zeolite) in a quartz cell with a flat bottom (88 ml) connected to a conventional vacuum system (10^{-6} Torr range). UV-irradiation of the catalysts in the presence of CO_2 (36 μmol, 7.8 Torr) and gaseous H_2O (180 μmol, 39.0 Torr) was carried out using a 75-W high-pressure Hg lamp ($\lambda > 250$ nm) at 328 K.

The photocatalytic reactions of NO molecules were carried out with the catalysts (150 mg) in a quartz cell with a flat bottom (60 ml) connected to a conventional vacuum system (10^{-6} Torr range). UV-irradiation of the catalysts in the presence of NO (7.8 μmol) was carried out using a 75-W high-pressure Hg lamp ($\lambda > 280$ nm) at 275 K.

The reaction products collected in the gas phase were analyzed by gas chromatography.

4. 2. 3 Characterization

The XAFS spectra (XANES and EXAFS) were measured at the BL-9A facility [12] of the Photon Factory at the National Laboratory for High-Energy Physics, Tsukuba. A Si(111) double crystal was used to

monochromatize the X-rays from the 2.5 GeV electron storage ring. The normalized spectra were obtained by a procedure described in previous literature [13] and Fourier transformation was performed on k^3- weighted EXAFS oscillations in the range of 3-10 $Å^{-1}$. The curve-fitting of the EXAFS data was carried out by employing the iterative nonlinear least-squares method and the empirical backscattering parameter sets extracted from the shell features of titanium compounds.

4. 3 Results and Discussion

4. 3. 1 Characterization of Ti-Beta zeolites

Figure 4-1 shows the XANES spectra of the Ti-Beta zeolites. The XANES spectra of the Ti containing compounds at the Ti K-edge show several well-defined pre-edge peaks that are related to the local structures surrounding the Ti atom. These relative intensities of the preedge peaks provide useful information on the coordination number surrounding the Ti atom [14]. As shown in Fig. 4-1, both Ti-Beta(OH) and Ti-Beta(F) zeolites exhibit an intense single pre-edge peak. Because a lack of an inversion center in the regular tetrahedron structure causes an intense single pre-edge peak [15], the observation of this intense single pre-edge peak indicates that the titanium oxide species in the Ti-Beta zeolites has a tetrahedral coordination. The Ti-Beta(OH) and Ti-Beta(F) zeolites exhibit the pre-edge peaks having the same intensities and positions indicating that both zeolites have the same titanium coordination.

Figure 4-1 also shows the FT-EXAFS spectra of the zeolites and all data are given without corrections for phase shifts. Both Ti-Beta(OH) and Ti-Beta(F) zeolites exhibit only a strong peak at around 1.6 Å (uncorrected for the phase shift) which can be assigned to the neighboring oxygen atoms (a Ti-O bond), indicating the presence of the isolated titanium oxide species on these zeolites. From the results obtained by the curve-fitting analysis of the EXAFS spectra, it was found that the Ti-Beta zeolites consist of 4-coordinated titanium ions with an atomic distance of 1.84 Å for Ti-Beta(OH) and 1.83 Å for Ti-Beta(F).

The H_2O affinity of Ti-Beta zeolites can be evaluated by monitoring the H_2O adsorption isotherms. Figure 4-2 shows H_2O adsorption isotherms with increasing water vapor (P) relative to the saturated vapor pressure (P_0) on the Ti-Beta zeolites. These results indicate that the Ti-Beta(OH) and Ti-Beta(F) zeolites synthesized using a typical OH^- ion and F^- ion as the anion of the SDA exhibit hydrophilic and hydrophobic properties, respectively. The large molecule of SDA, N'-dibenzyl-4,4'-trimethylenebis (N-methylpiperidinium) dihydroxide, for the synthesis of Ti-Beta(OH) can be removed only by calcination leaving many defect sites in the zeolite pore [2]. On the other hand, it has been reported that Ti-Beta free of detect sites can be prepared by using TEAF as SDA [3]. This difference in the numbers of defect sites between these Ti-Beta zeolites generates the unique hydrophilic and hydrophobic properties, respectively.

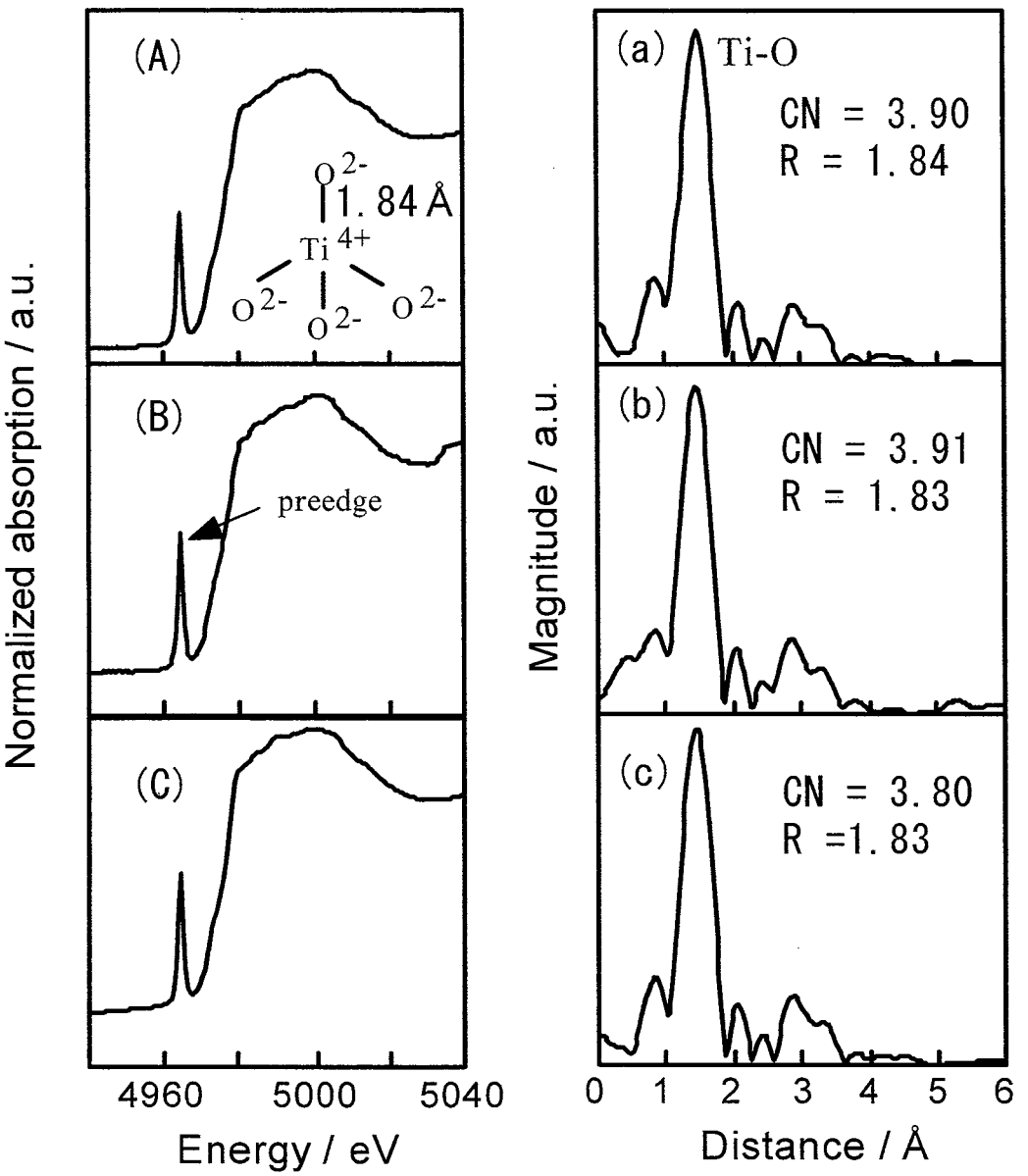

Figure 4-1. The Ti K-edge XANES (left) and FT-EXAFS (right) spectra of Ti-Beta(OH) (A, a), Ti-Beta(F) (B, b), and TS-1 (C, c). CN: coordination number, R: Ti-O bond distance (Å).

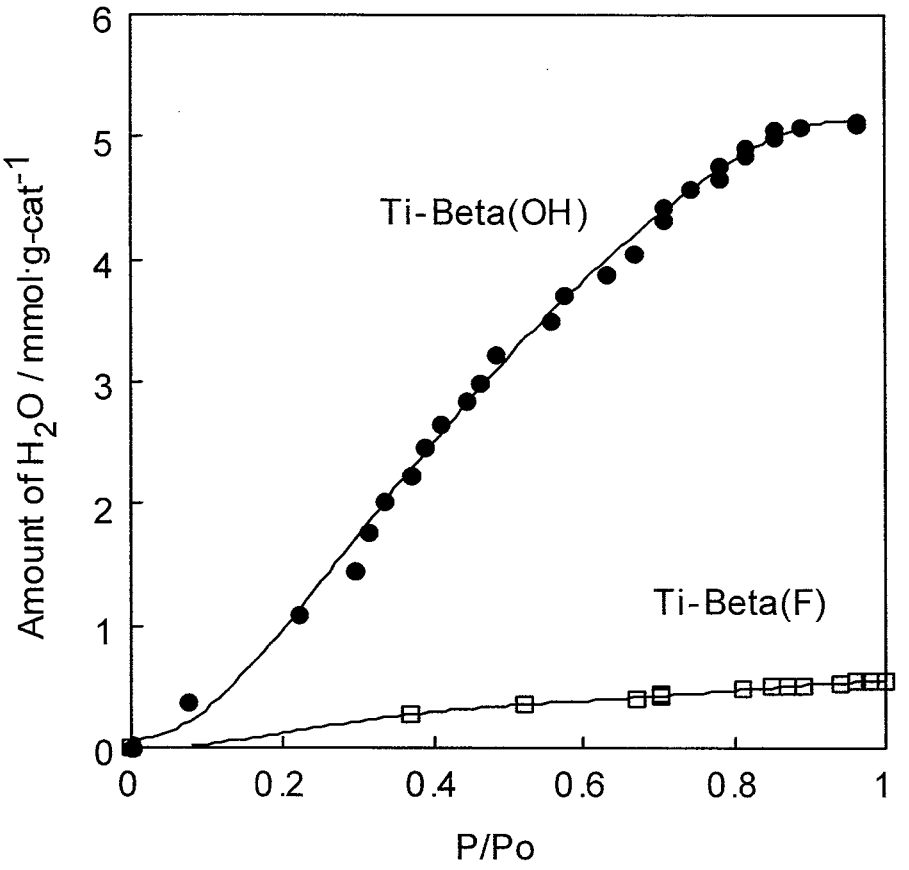

Figure 4-2. Adsorption isotherms for H_2O molecules at 298 K on the Ti-Beta(OH) and Ti-Beta(F) zeolites.

The photocatalytic degradation of 2-propanol diluted in water was investigated using the Ti-Beta zeolite photocatalysts. Some amounts of 2-propanol were adsorbed on the photocatalyst without light irradiation, and then the photocatalytic reaction proceeds with the UV-irradiation. As shown in Fig. 4-3, the concentration of 2-propanol decreased and acetone increased as the intermediate, finally 2-propanol and acetone were degradated into CO_2 and H_2O. The other by-products were not observed.

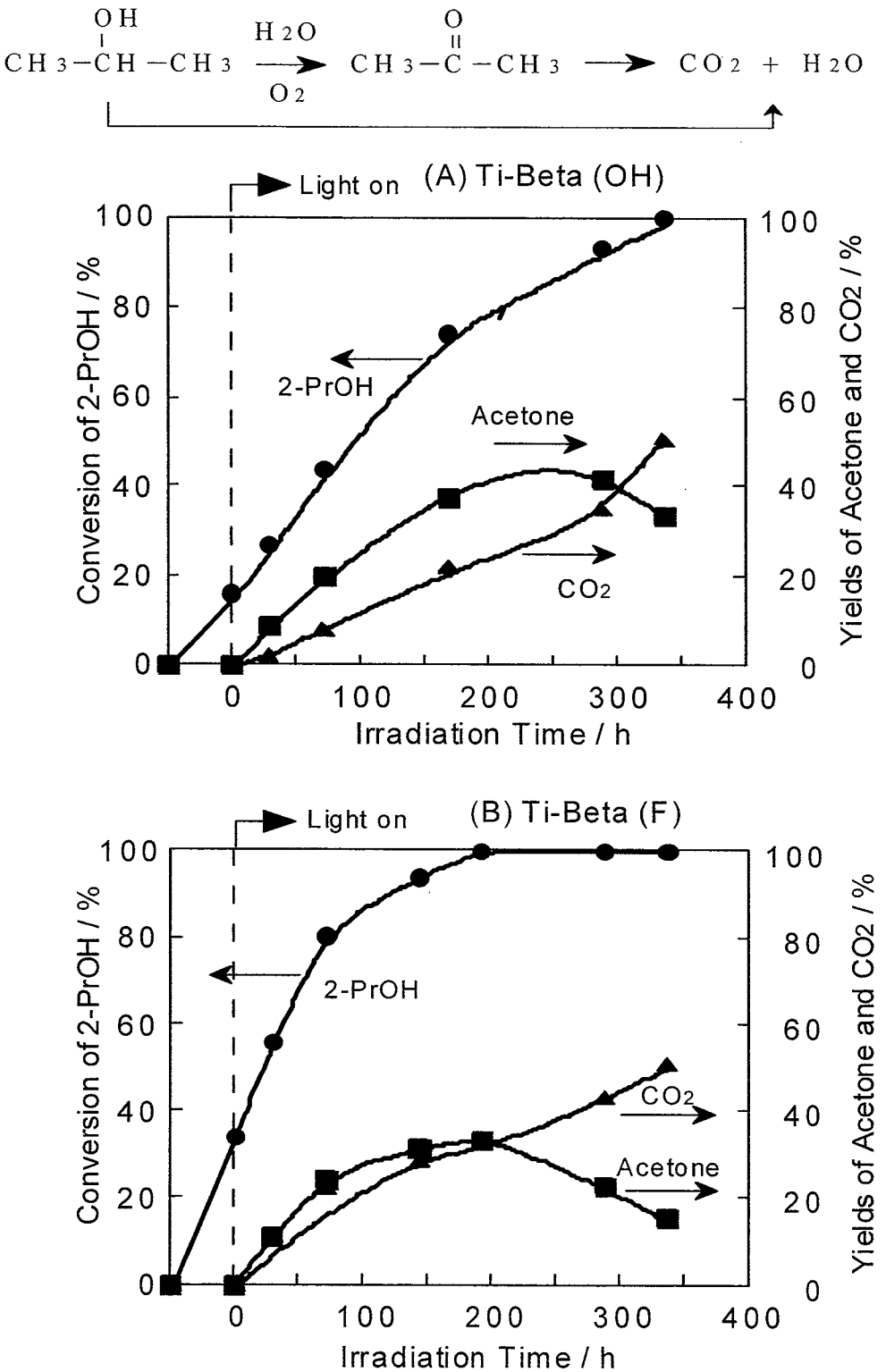

Figure 4-3. Reaction time profiles of the photocatalytic oxidative degradation of 2-propanol diluted in water on (A) Ti-Beta(OH) and (B)Ti-Beta(F) zeolites.

Figure 4-4 shows the adsorption properties and photocatalytic reactivities of Ti-Beta zeolites and TiO_2 powder (P-25) photocatalysts for the degradation of 2-propanol in water. Ti-Beta zeolites indicate the higher ability for 2-propanol adsorption and higher efficiency for the photocatalytic degradation than commercial TiO_2 powder (P-25) photocatalyst. Among the Ti-Beta zeolites, the amount of adsorbed 2-propanol on Ti-Beta(F) is higher than that of Ti-Beta (OH), indicating that efficient adsorption of organic compounds in the aqueous solutions can be realized by fluoride-modified hydrophobic zeolite. Because the Ti-Beta(F) exhibited the photocatalytic reactivity higher than Ti-Beta(OH), it can be also found that the more highly adsorption, the more efficiently photocatalytic reactivities were promoted.

UV-irradiation of powdered TiO_2 and Ti-Beta zeolite catalysts in the presence of a mixture of CO_2 and H_2O led to the evolution of CH_4 and CH_3OH in the gas phase at 328 K. The yields of these photoformed products increased linearly against the UV-irradiation time, indicating the photocatalytic reduction of CO_2 with H_2O on the catalysts.

The specific photocatalytic reactivity for the formation of CH_4 and CH_3OH are shown in Fig. 4-5. The photocatalytic reduction of CO_2 with H_2O to produce CH_4 and CH_3OH was found to proceed in the gas phase at 323 K with different reactivity and selectivity on hydrophilic Ti-Beta(OH) and hydrophobic Ti-Beta(F) zeolites. The higher reactivity for the formation of CH_4 observed with Ti-Beta(OH) and the higher selectivity for the formation of CH_3OH observed with the Ti-Beta(F) may be attributed to the different abilities of zeolite pores on the H_2O affinity. These results

suggest that the hydrophilic-hydrophobic property of surface of zeolite cavities is one of important factors for the selectivity in the photocatalytic reduction of CO_2 and H_2O.

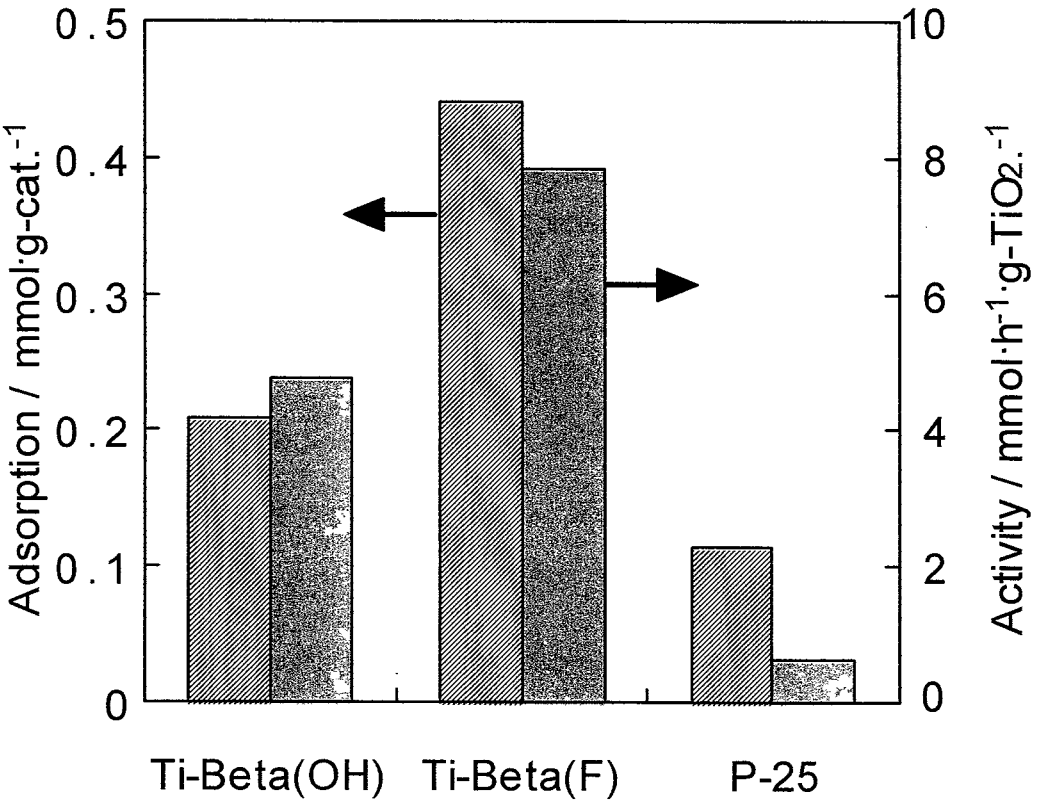

Figure 4-4. The adsorption properties and photocatalytic reactivities of Ti-Beta zeolite and TiO_2 powder (P-25) photocatalysts for the degradation of 2-propanol in water.

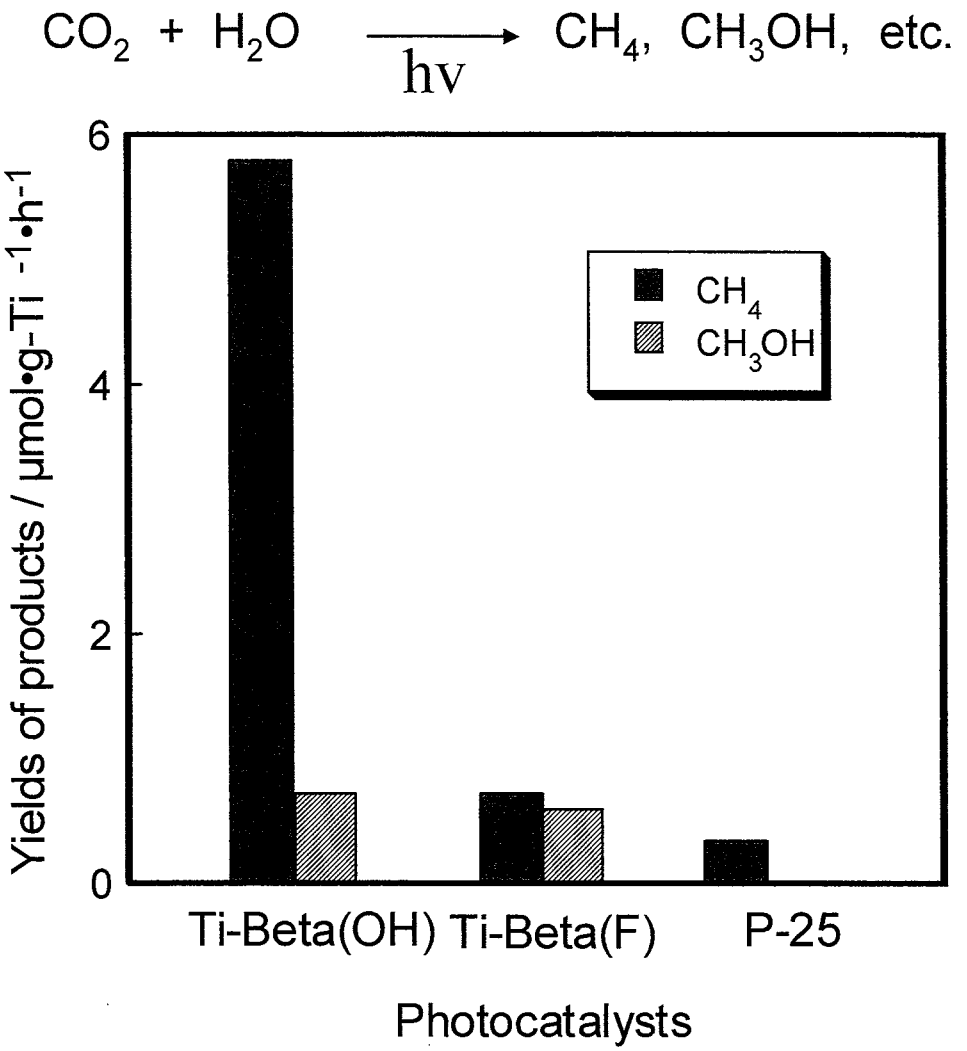

Figure 4-5. The yields of CH_4 and CH_3OH in the photocatalytic reduction of CO_2 with H_2O at 323 K as the gas phase reaction.

UV-irradiation of the powdered TiO_2 and the Ti-Beta zeolites in the presence of NO were found to lead to the evolution of N_2, O_2 and N_2O in the gas phase at 275 K with different yields and different product selectivity. The efficiency and selectivity for the formation of N_2 strongly depend on the type of catalysts as shown in Fig. 4-6. The Ti-Beta zeolite exhibits a high

reactivity and a high selectivity for the formation of N_2 while the formation of N_2O was found to be the major reaction on the powder TiO_2 catalyst.

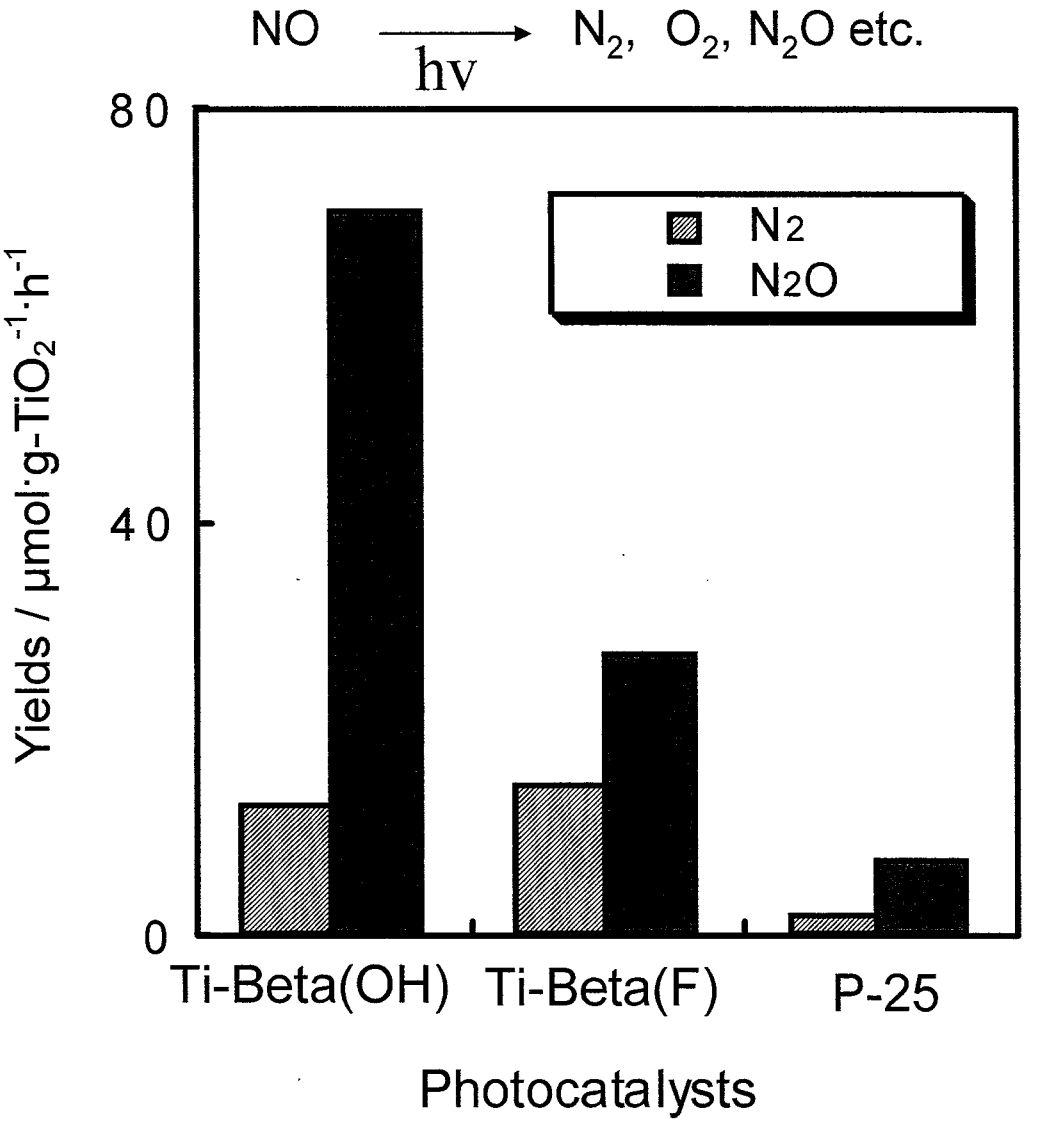

Figure 4-6. The yields of N_2 and N_2O in the photocatalytic decomposition of NO at 273 K as the gas phase reaction.

As shown in Figs. 4-5 and 4-6, the Ti-Beta(OH) zeolite exhibits the higher photocatalytic reactivity than the Ti-Beta(F) for the gas-phase reactions; CO_2 reduction with H_2O and NO decomposition. On the other

hand, Ti-Beta(F) exhibited the higher reactivity than Ti-Beta(OH) as shown in Figs. 4-3 and 4-4 for the liquid-phase reaction; degradation of 2-propanol diluted in water. These results suggest that the photocatalytic reactivity of active site of Ti-oxide moieties in zeolite is higher on the Ti-Beta(OH) than the Ti-Beta(F). However, in the liquid-phase reaction, the hydrophobic surface property of Ti-Beta(F) zeolite can realize the efficient adsorption of organic compounds and promote the photocatalytic degradation significantly. These results suggest that combination of photocatalyst and the hydrophobic porous supports is suitable for the liquid-phase photocatalytic reaction.

4. 3. 2 Characterization of imp-TiO_2/HMS(F)

The XRD patterns of the fluoride-modified hydrophobic mesoporous silica (HMS(F)) exhibited well-resolved peak typical of hexagonal structure of the HMS mesoporous molecular sieves having pores larger than 20 Å [11]. With increase the content of fluoride, the peak shifted to the lower angle with decrease in its intensity, suggesting the mesoporous hexagonal structure was distorted. The BET surface area of HMS(F) catalysts were measured by monitoring the physical adsorption of N_2 at 77K: the values are 682 m^2g^{-1} (HMS), 581 (HMS(F1)), 487 (HMS(F2)) and 258 (HMS(F3)). The surface area decreased with increase the content of fluoride.

Figure 4-7 shows the adsorption isotherm of H_2O molecules at 298 K obtained over various HMS(F) catalysts, indicating that the amount of adsorbed H_2O molecules decreases with increasing the content of fluoride in

the HMS(F) mesoporous silica. The values of H_2O adsorption ability per unit surface area of catalysts at $P/P_0=1$ are 7.1 mmol/m^2-cat. (HMS), 2.6 (HMS(F1)), and 1.5 (HMS(F3)). This shows that fluoride-modified mesoporous silica can be hydrophobilized by the fluoride-modifications.

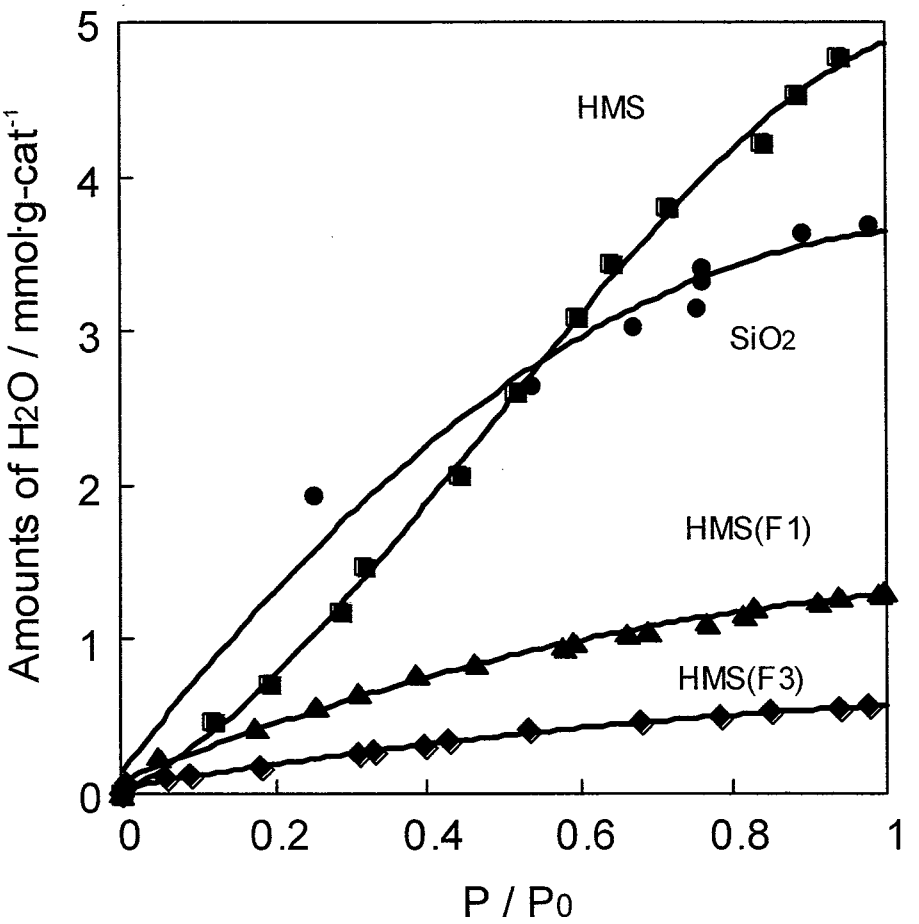

Figure 4-7. Adsorption isotherms for H_2O molecules at 298 K on the HMS(F) mesoporous silica.

Figure 4-8 shows the XAFS spectra of the imp-TiO_2/HMS catalysts. The XANES spectra of these catalysts at the Ti K-edge exhibit the preedge peak branched off into three distinct weak peaks. The FT-EXAFS spectra

exhibit the existence of the peaks attributed to the neighboring O atoms (Ti-O) and the neighboring Ti atoms (Ti-O-Ti). These XAFS results indicate that the TiO_2 loaded on the mesoporous silica exists in the fine particles of anatase TiO_2 crystalline as main component [15].

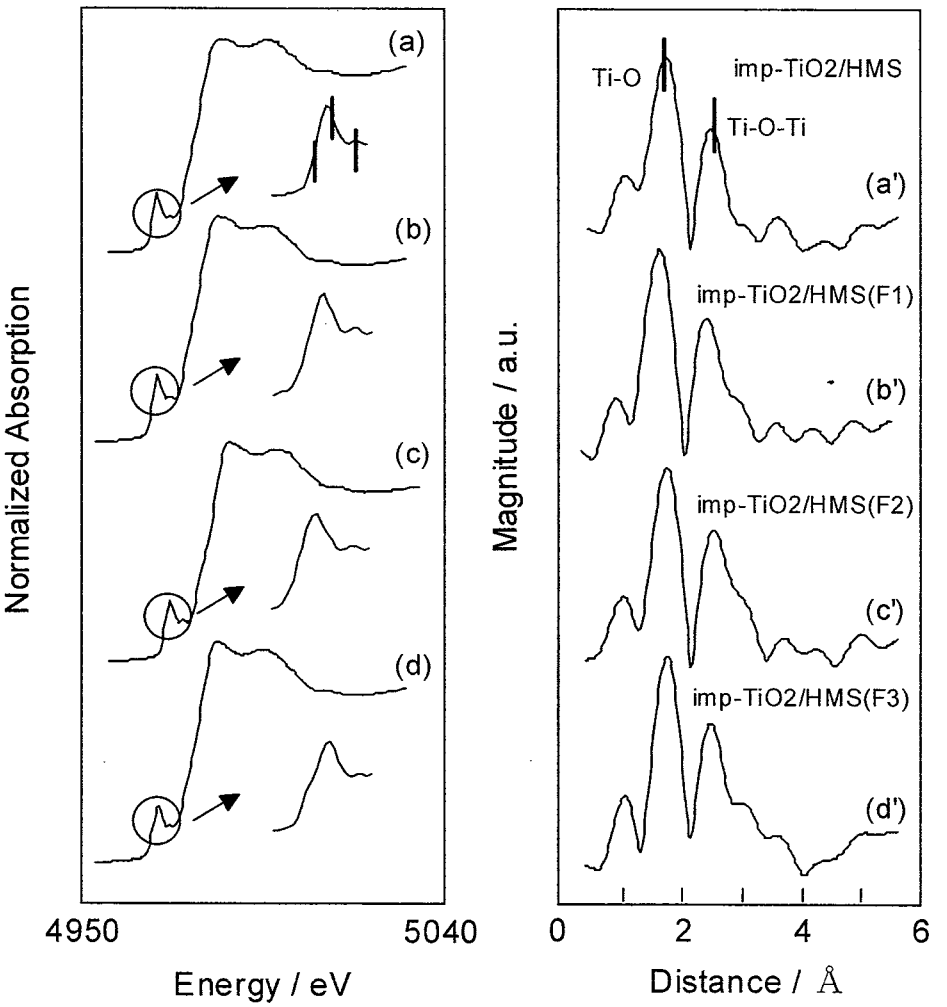

Figure 4-8. XANES(a-d) and FT-EXAFS(a'-d') spectra of the imp-TiO_2/HMS(F) photocatalysts.

The photocatalytic degradation of alcohol diluted in water was investigated using the imp-TiO_2/HMS(F) photocatalysts. Some amounts of 2-propanol were adsorbed on the photocatalyst without light irradiation, and then the photocatalytic reaction proceeded with the UV-irradiation. The concentration of 2-propanol decreased and acetone increased as the intermediate, finally 2-propanol and acetone were degradated into CO_2 and H_2O.

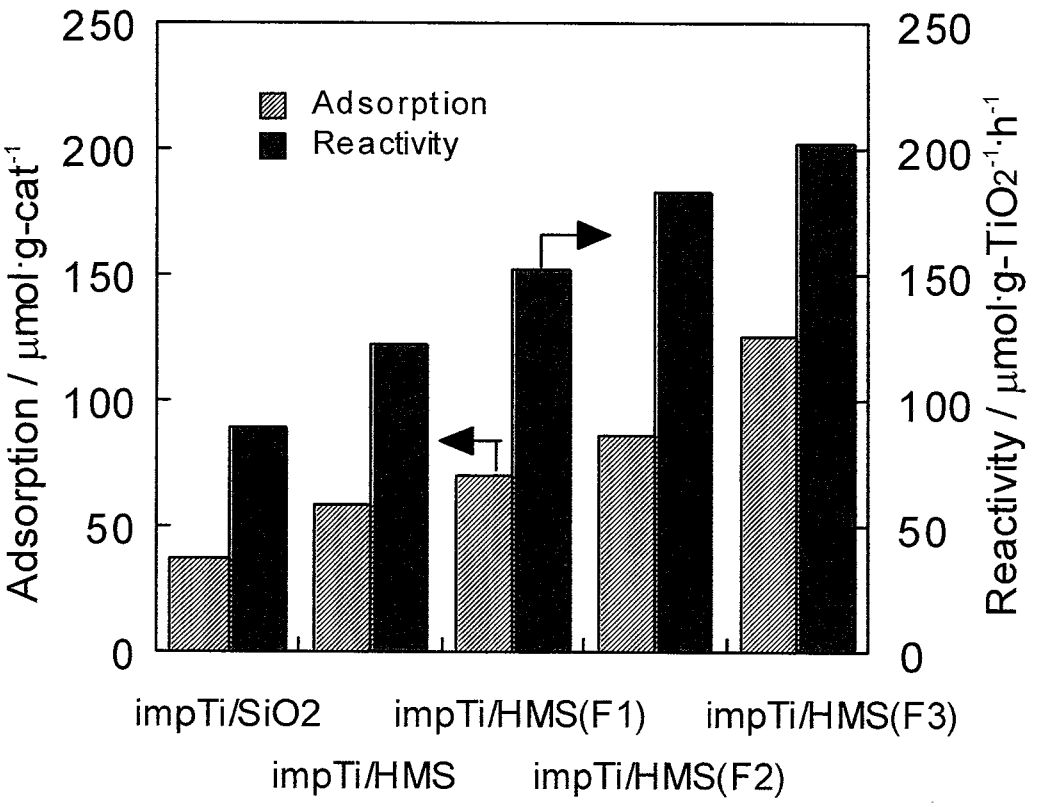

Figure 4-9. The adsorption properties and photocatalytic reactivities of imp-TiO_2/HMS(F) photocatalysts for the degradation of 2-propanol in water.

Figure 4-9 shows the adsorption properties and photocatalytic reactivities of imp-TiO_2/HMS(F) photocatalysts for the degradation of 2-propanol in water. The amount of adsorbed 2-propanol increased with increasing the amount of fluoride in HMS(F), indicating that efficient adsorption of organic compounds in their aqueous solutions can be realized by hydrophobilizing the support. Furthermore, it can be found that the more highly adsorption, the more efficiently photocatalytic reactivities were promoted on HMS(F).

4. 4 Conclusion

Ti-containing zeolites are good candidates as efficient photocatalysts. It has been revealed that the Ti-Beta zeolites synthesized in the media of OH^- ion and F^- ion exhibit hydrophilic and hydrophobic properties, respectively. The hydrophilic Ti-Beta(OH) and the hydrophobic Ti-Beta(F) exhibited the photocatalytic efficiency in the different manor for the gas-phase and liquid-phase reactions. Ti-Beta(F) exhibited a higher reactivity for the degradation of 2-propanol as compared to Ti-Beta(OH) due to the higher affinity of the 2-propanol molecules for adsorption in aqueous solutions, which was induced by the fluoride-modified hydrophobic surface.

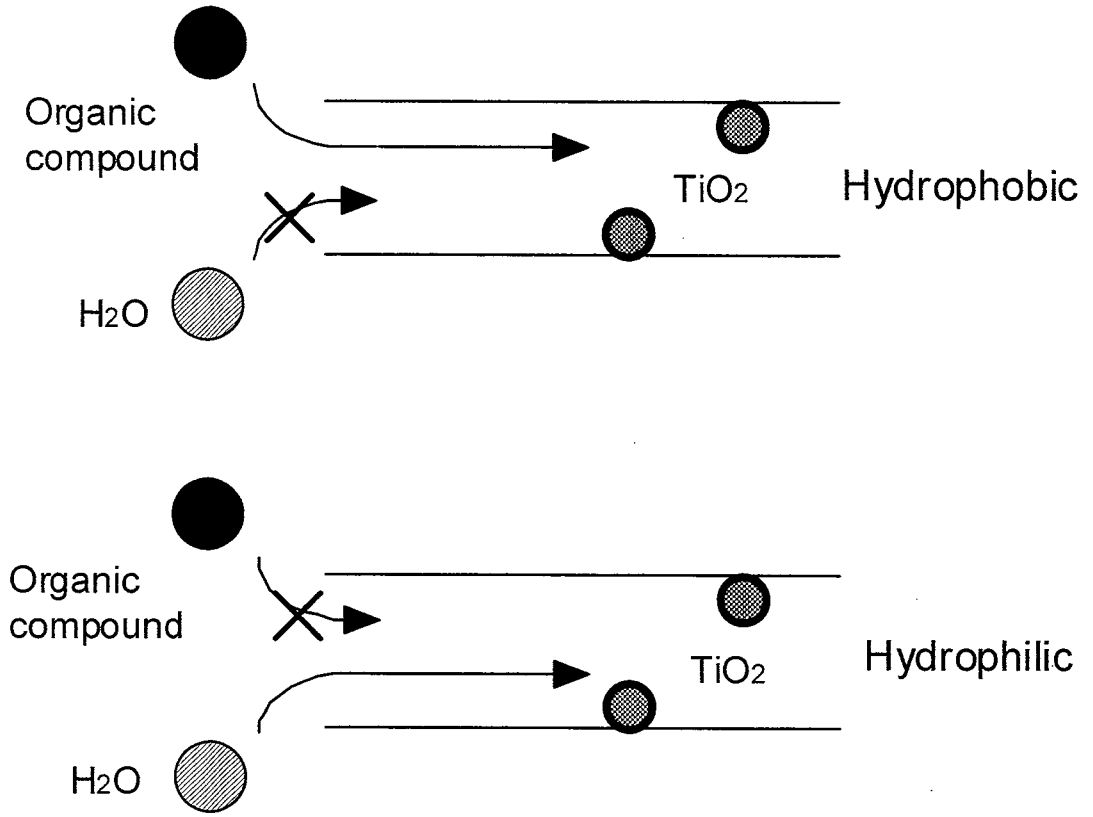

Scheme 4-1. The difference of the adsorption of H_2O or organic compound on the system of TiO_2 photocatalyst and hydrophilic-hydrophobic adsorbents in the liquid phase.

The TiO_2 photocatalysts loaded on the fluoride-modified hydrophobic mesoporous silica also exhibited the highly selective adsorption of organic compounds in the liquid phase. The hydrophobic surface of HMS(F) supports was suitable for the adsorption of organic compounds and the larger amount of adsorbing organic compounds on the imp-TiO_2/HMS(F) led to the higher reactivity for photocatalytic degradation. The combination of the porous adsorbents with fluoride-modified hydrophobic surface and titanium

oxide photocatalyst is a good candidate as the efficient system for the degradation of organic pollutants diluted in water as shown in Scheme 4-1.

4. 5 References

[1] H.Yamashita and M. Anpo, *Current Opinion in Solid State & Maters. Sci.*, 7, 471 (2004).

[2] T. Takewaki, S. J. Hwang, H. Yamashita, M. E. Davis, *Micropor. Mesopor. Mater.*, 32, 265 (1999).

[3] M. A. Camblor, A. Corma, P. Esteve, M. Martines, S. Valencia, *Chem. Commun.*, 795 (1997).

[4] K. Ikeue, H.Yamashita, T. Takewaki, M. Anpo, *J. Phys. Chem. B*, **105**, 8350 (2001).

[5] S. Horikoshi, H. Hidaka, N. Serpone, *Env. Sci. Tech.*, **36**, 1357 (2002).

[6] C. Minero, G. Mariella, V. Maurino, E. Pelizzetti, *Langmuir*, **16**, 8964 (2000).

[7] N. Takeda, T. Torimoto, S. Sampath, S. Kuwabata, H. Yoneyama, *J. Phys. Chem.*, **99**, 9986 (1995).

[8] H. Yamashita, Y. Ichihashi, M. Harada, G. Stewart, M.A. Fox, M. Anpo, *J. Catal.*, **158**, 97 (1996).

[9] H. Yamashita, S. Kawasaki, Y. Ichihashi, M. Harada, M. Anpo, G. Stewart, M. A. Fox, C. Louis, M. Che, *J. Phys. Chem. B*, 102, 5870 (1998).

[10] H. Yamashita, M. Honda, M. Harada, Y. Ichihashi, M. Anpo, Y. Hatano, *J. Phys. Chem. B*, 102, 10707 (1998).

[11] W. Zhang, P. T. Tanev, T. J. Pinnavaia, *J. Chem. Soc., Chem. Commun.*, 979 (1996).

[12] M. Nomura and A. Koyama, *J. Synchrotron Rad.*, 6, 182 (1999).

[13] H. Yamashita, M. Matsuoka, K. Tsuji, Y. Shioya, M. Anpo, *J. Phys. Chem.*, 100, 397 (1996).

[14] J. M. Thomas and G. Sankar, *J. Synchrotron Rad.*, 8, 55 (2001).

[15] H. Yamashita, Y. Ichihashi, M. Anpo, C. Louis, M. Che, *J. Phys. Chem.*, 100, 16041 (1996).

Chapter 5

Degradation of Organic Compounds on TiO_2 Photocatalysts Prepared by the Hydrothermal Method in the Presence of NH_4F

5. 1 Introduction

Photocatalytic degradation of organic pollutants diluted in water using TiO_2 is of vital interest. TiO_2 is a promising photocatalyst because of low cost, nontoxity as well as strong oxidation ability under UV-light irradiation [1]. To realize the practical application of TiO_2 photocatalytic system, the various modifications of TiO_2 have been investigated to increase the photocatalytic activity under not only UV-light but also visible-light irradiation [2]. Because the highly crystallized TiO_2 without the defect sites were found to be effective photocatalyst, the hydrothermal synthesis of TiO_2 has been applied using the organic solvents [3]. The implantation of metal cations, such as Fe, Cr, and V, has been found to be effective to modify TiO_2 into the visible-light sensitive photocatalyst [4]. Recently, as a cheep method, Asahi et al. also demonstrated that the doping of nitrogen into TiO_2 provided the visible-light responsibility [5]. On the other hand, the doping of F^- ion within the TiO_2 lattice using NaF as a fluorine source showed the enhancement in the photocatalytic activity [6-8]. The introduction of F^- ion is also promising to reduce the hydrophilic nature of TiO_2 particle surface, which could enhance the affinity of TiO_2 surface toward organic compounds by the replacement of surface ·OH group by F^-. The modification of hydrophilic TiO_2 surface also could be achieved by HF or F_2 treatment.

In the present study, TiO_2 fine powder was synthesized by hydrothermal condition in the presence of NH_4F (HT-TiO_2). The effects of

NH_4F on the photocatalysis of HT-TiO_2 have been investigated for the photocatalytic degradation of alcohols (*i*-BuOH, 2-PrOH) diluted in water under UV-light and visible-light irradiation.

5. 2 Experimental

TiO_2 fine powder was synthesized by the hydrothermal method using tetraisopropyl orthotitanate (TPOT: $Ti(OC_3H_7)_4$) as the starting material in the mixed NH_4F-H_2O-ethanol solution with molar ratios of (Ti : H_2O : EtOH =1 : 5 : 5). NH_4F/Ti molar ratios in the starting mixtures were 0/1, 0.25/1, and 1/1. The above mixtures were transferred into an autoclave and kept at 433 K for 48 h. After centrifugation, washing, drying, and calcination at 823 K for 5 h, TiO_2 powders were obtained. The products were denoted as HT-TiO_2(0), HT-TiO_2(0.25), and HT-TiO_2(1), respectively. TiO_2 was also prepared by the conventional sol-gel method with a mixture of TPOT, H_2O, and EtOH (1 : 5 : 5) after stirring at room temperature for 24 h, and then heating at 358 K for 24 h. After centrifugation, drying, and calcination at 823 K for 5 h, the sol gel-TiO_2 was obtained.

X-ray diffraction patterns of all samples were measured using Rigaku RINT2500 diffractometer with Cu Kα radiation. By using an ASAP 2000 system (Shimadzu), the BET method was applied for the determination of the specific surface area. The diffuse reflectance absorption spectra were recorded with Shimadzu UV-2200A

photospectrometer. X-ray photoelectron spectrum was recorded with JEOL microprobe system using the Mg Kα line.

The photocatalytic activity of TiO_2 was evaluated by the photodegradation of alcohol (*i*-BuOH, 2-propanol) diluted in water. 0.05 g of catalyst was placed in a quartz cell with 25 ml of aqueous alcohol solution (2.61 $mmol \cdot l^{-1}$) . After stirring under dark conditions for 30 min, the solution was bubbled by oxygen for another 30 min. Then the solution was irradiated under UV-light ($\lambda > 280$ nm) or visible-light from a 100 W high-pressure Hg lamp. The reactions were monitored by gas chromatography analysis (GC-14B, Shimadzu). Water adsorption isotherms of the catalysts were measured at 293 K using a conventional vacuum system.

5. 3 Results and Discussion

Figure 5-1 shows the XRD patterns of the hydrothermally synthesized TiO_2 (HT-TiO_2) and the sol-gel synthesized TiO_2 (sol-gel TiO_2) calcined at 823 and 923 K. The HT-TiO_2 catalysts calcined at 823 K show sharp peaks corresponding to only anatase phase of TiO_2 but no other phases such as rutile and brookite can be detected. On the contrary, additional peaks corresponding to the rutile phase at 27.5 and 36.0° were observed in the sol-gel TiO_2. The HT-TiO_2 catalysts exhibit the higher intensity of (101) peak due to the anatase phase than that of the sol-gel TiO_2, indicating that the TiO_2 with the high crystallinity can be synthesized using

the hydrothermal synthesis.

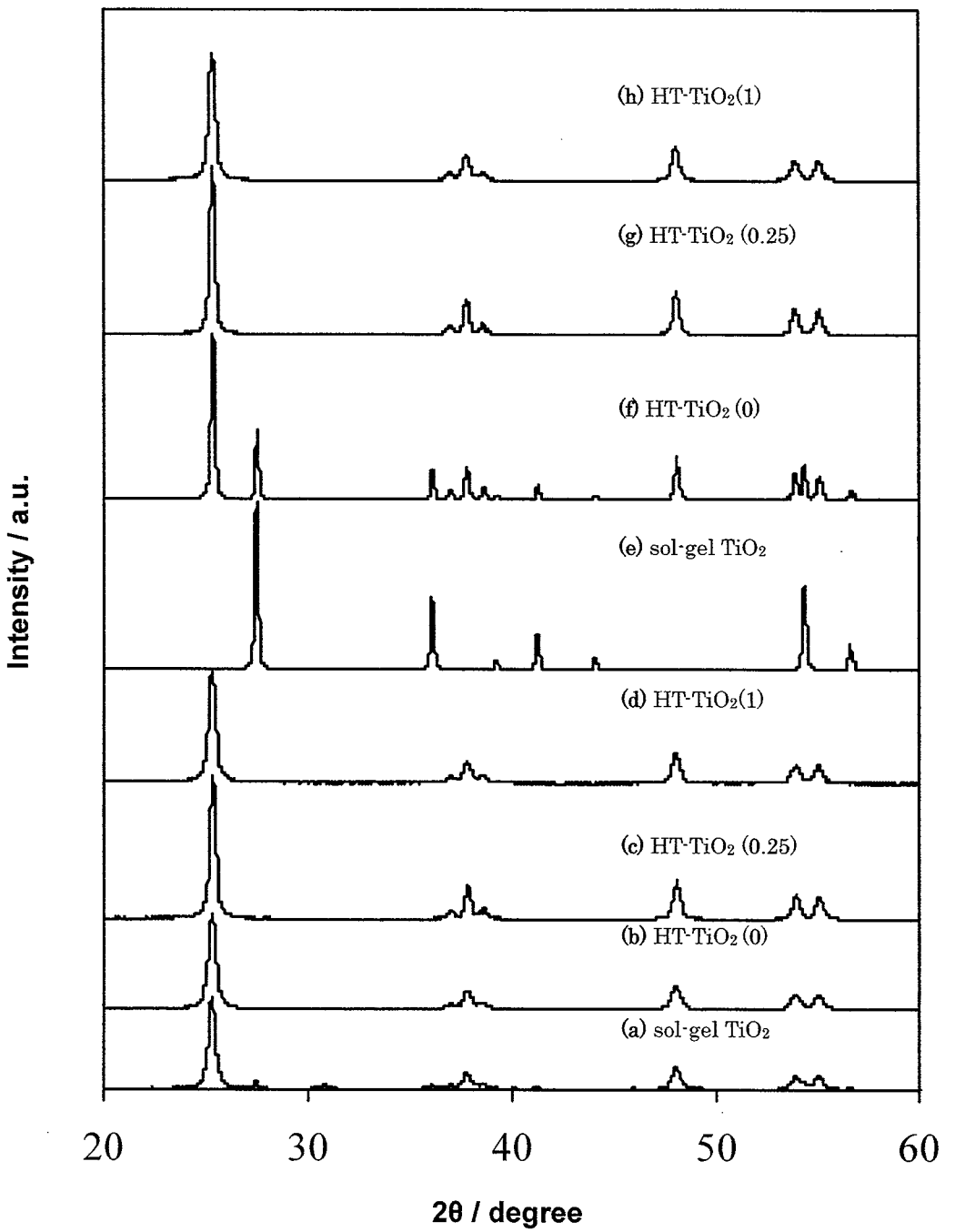

Figure 5-1. XRD patterns of TiO_2 prepared by the sol-gel method and hydrothermally synthesized HT-TiO_2 samples with different amount of NH_4F after calcination at 823 K (a-d) and 923 K (e-h).

Among the catalysts, HT-TiO_2 (0.25) exhibits the highest intensity of (101) peak due to anatase phase in the both cases of the calcinations at 823 and 923 K. The BET surface are of these catalysts were measured as 55 m^2g^{-1} (HT-TiO_2 (0)), 33 m^2g^{-1} (HT-TiO_2 (0.25)), and 47 m^2g^{-1} (HT-TiO_2 (1)), respectively. The results of the BET surface areas reflected the crystallinity estimated from XRD measurement. The surface area decreased with increasing the crystallinity.

The XRD patterns of HT-TiO_2 and sol-gel TiO_2 calcined at 923 K are also shown in Fig. 1. The rutile phase was dominant in the sol-gel TiO_2. The HT-TiO_2 (0) showed the formation of the mixture of anatase and rutile phases. But with HT-TiO_2 (0.25), and HT-TiO_2 (1)) the phase transfer to rutile was completely suppressed and all peaks could be assigned as the anatase phase of TiO_2 crystalline. It should be noted that the hydrothermal synthesis of TiO_2 from TPOT in the presence of NH_4F inhibit the phase transformation from anatase to rutile with increasing calcination temperature. F^- ion doping should enhance the crystallization of anatase phase and suppress the crystallization into rutile phase.

The F_{1s} XPS spectra of the present catalysts were measured. It was found that the F_{1s} band with binding energy at around 688 eV corresponding to the F^- ions in the TiO_2 lattice can be observed with the HT-TiO_2 (F1), while that at 684 eV is ascribed to the adsorbed F^- ions on TiO_2 surface. Although the intensity of the F_{1s} was low in the HT-TiO_2 (F1), one major peak due to the F^- ions in the TiO_2 lattice was observed. On the other hand, no noticeable signals assignable to N_{1S} binding energy could be

observed in the HT-TiO_2 (F1), suggesting that N atoms originating from the NH_4F scarcely present.

The water adsorption isotherms of HT-TiO_2 catalysts are shown in Figure 5-2. The amount of adsorbed H_2O molecules decreased on the HT-TiO_2 (0.25) than HT-TiO_2 (0), which may indicated that the hydrophobic properties were generated by the replacement of -OH group by F^-. The result indicates that the TiO_2 synthesized in the presence of NH_4F demonstrated the higher hydrophobic property than pure TiO_2.

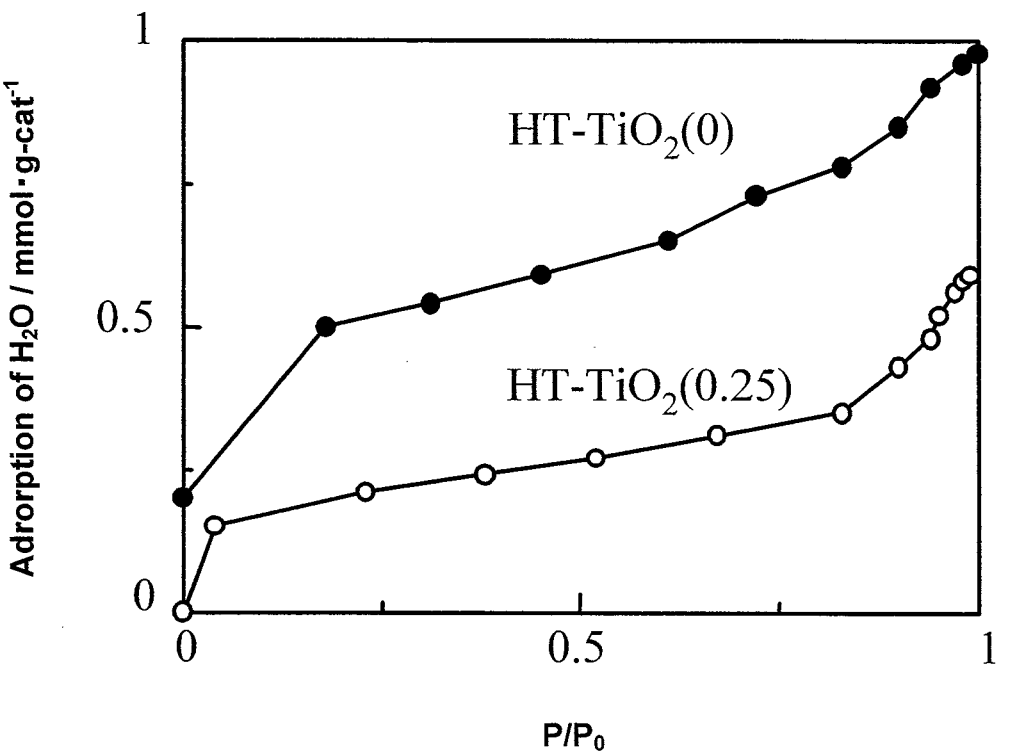

Figure 5-2. H_2O adsorption of the HT-TiO_2 samples calcined at 823 K.

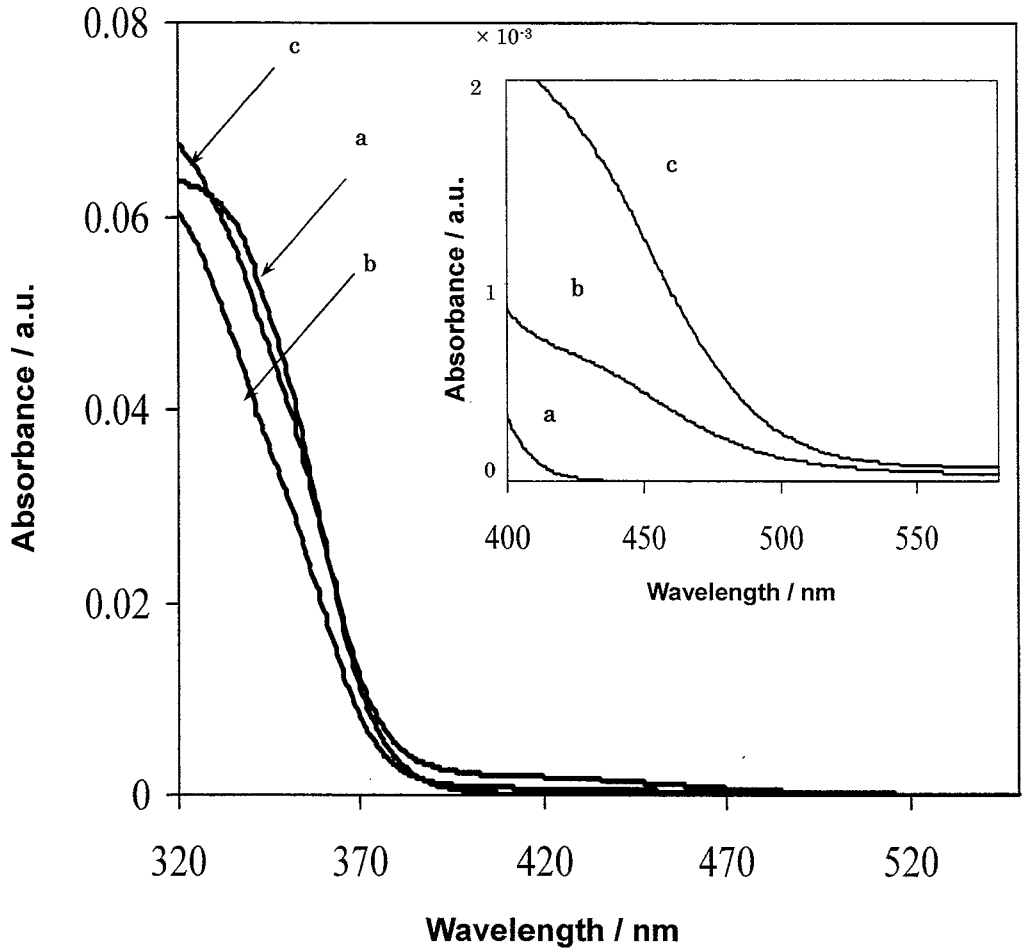

Figure 5-3. UV-vis spectra of (a) HT-TiO_2 (0), (b) HT-TiO_2 (0.25), and (c) HT-TiO_2 (1).

Figure 5-3 shows the UV-vis absorption spectra of the HT-TiO_2 catalysts. While the HT-TiO_2(0) catalyst exhibits similar absorption edge to that of the pure anatase TiO_2, the HT-TiO_2(0.25) and HT-TiO_2(1) catalysts show a shift to visible-light range (> 430 nm) in the absorption band. This observation indicates that the synthesis in the presence of NH_4F clearly influenced on the light absorption characteristics of HT-TiO_2 catalysts. It has been reported that the F^- ions doping does not cause a shift in the

fundamental absorption edge of TiO_2 with the theoretical band calculations for F^- ions doped TiO_2 [9]. Although the author could not detect the nitrogen atoms by the XPS analysis, an extremely small amount of N contamination from NH_4F in the HT-TiO_2(0.25) and HT-TiO_2(1) catalysts may make the band edge shift to the longer wavelength.

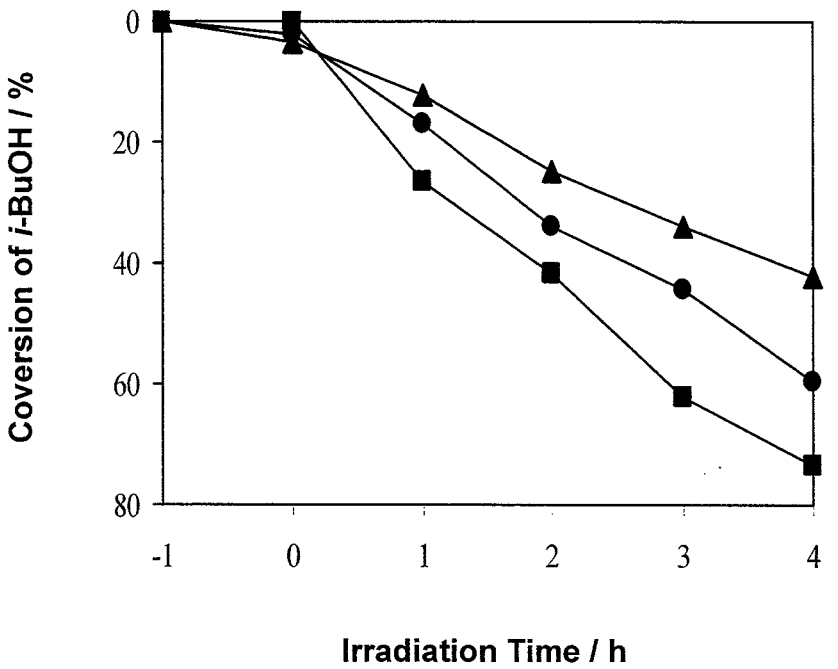

Figure 5-4. Photocatalytic degradation of *i*-BuOH diluted in water on HT-TiO_2 (0) (●), HT-TiO_2 (0.25)(■), and HT-TiO_2 (1)(▲).

The photocatalytic reactivity for the degradation of iso-butanol diluted in water was investigated on HT-TiO_2 catalysts and the time profiles of reactions are shown in Fig. 5-4. The TH-TiO_2(0.25) catalyst exhibits the highest photocatalytic reactivity under UV-light irradiation among the catalysts and also exhibits the reactivity for the degradation of 2-propanol

even under visible-light irradiation as shown in Fig. 5-5. In the case of the HT-TiO_2(0.25), high crystallinity of the anatase phase, the hydrophobic surface property and the photo absorption ability in the wider range are factors for the high activity. On the other hand, the HT-TiO_2(1) exhibits apparently a decrease in photocatalytic activity. An excessive F^- doping in the HT-TiO_2(1) maybe play a negative role in photocatalysis, because such sites lead the charge recombination in bulk which causes the lower photocatalytic activity.

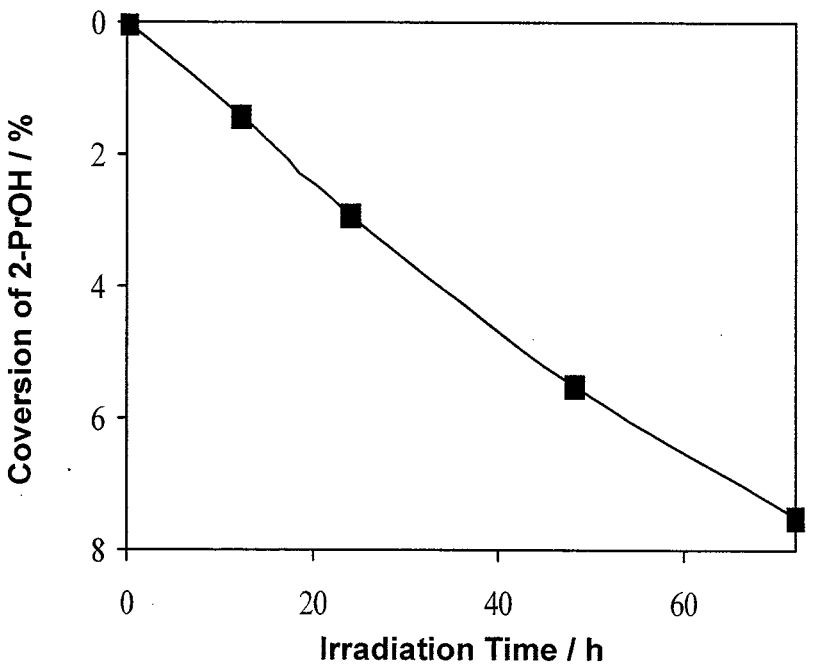

Figure 5-5. Photocatalytic degradation of 2-PrOH diluted in water on HT-TiO_2 (0.25) under visible light orradiation (λ >430 nm).

5. 4 Conclusions

TiO_2 photocatalysts (HT-TiO_2) were synthesized by the hydrothermal method from tetraisopropyl orthotitanate (TPOT) in the presence of NH_4F with different NH_4F/Ti molar ratios. The formation of well-crystallized anatase phase of TiO_2 and suppression of phase transition to rutile were observed even at high calcination temperature. The photocatalytic activities were apparently affected by crystallinity of TiO_2 phase depending on the amount of employed NH_4F. The HT-TiO_2 catalyst with high F^- ion contents exhibited absorption in the range of visible-light. The HT-TiO_2 catalysts synthesized with the moderate amount of NH_4F exhibited efficient photocatalytic activity for the degradation of alcohol diluted in water under both UV-light and visible-light irradiation.

5. 5 References

[1] S. Horikoshi, H. Hidaka, N. Serpone, *Environ. Sci. Tech.*, 36, 1357 (2002).

[2] M.R. Hoffmann, S.T. Martin, W.Y. Choi, D.W. Bahnemann, *Chem.Rev.*, 95, 69 (1995).

[3] S. Murakami, H. Kominami, Y. Kera, S. Ikeda, H. Noguchi, K. Uosaki, B. Ohtani, *Res. Chem. Intermed.*, 33, 285 (2007).

[4] H.Yamashita and M. Anpo, *Catal. Surv. Asia*, 8, 35 (2004).

[5] R. Asahi, T. Morikawa, T. Ohwaki, K. Aoki, Y. Taga, *Science*, 293, 269 (2001).

[6] J. S. Park and W. Choi, Langmuir, 20, 11523 (2004).

[7] J.C. Yu, J. Yu, W. Ho, Z. Jiang, L. Zhang, *Chem. Mater.*, 14, 3808 (2002).

[8] T.K. Pong, J. Besida, T.A. O'Donnell, D.G. Wood, *Ind. Eng. Chem. Res.*, 34, 308 (1995).

[9] T. Morikawa, R. Asahi, T. Ohwaki, K. Aoki, Y. Taga, *Jpn. J. Appl. Phys.*, 40, 561 (2001).

Chapter 6

Summary and General Conclusions

6. 1 Summary

6. 1. 1 Summary of Chapter 2

Titanium-Silicon (Ti/Si) binary oxides having different Ti contents were prepared by the sol-gel method and used as photocatalysts. The photocatalytic reactivity of these catalysts was investigated as a function of the Ti content for the liquid-phase oxidation of 1-octanol to 1-octanal, and it was found to be dramatically enhanced in regions of lower Ti content. Further, the photocatalytic reactivity and selectivity of these catalysts were investigated as a function of the Ti content for the Hydrogenation and Hydrogenolysis of CH_3CCH with H_2O, and it was found that the hydrogenolysis reaction (C_2H_6 formation) was predominant in regions of low Ti content, while the hydrogenation reaction (C_3H_6 formation) proceeded in regions of high Ti content. In situ photoluminescence, UV-vis reflectance, FT-IR, ESR, XAFS, XRD, and XPS spectroscopic investigation of these Ti/Si binary oxides indicated that the titanium oxide species are highly dispersed in the SiO_2 matrixes and exist in a tetrahedral coordination exhibiting a characteristic photoluminescence spectrum due to the radiative decay from the charge-transfer excited state of the tetrahedrally coordinated titanium oxide species. The good parallel relationship between the yield of the photoluminescence and the specific photocatalytic reactivity of the Ti/Si binary oxides as a function of the Ti content clearly indicates that the high photocatalytic reactivity of the Ti/Si binary oxides having a low Ti content is

associated with the high reactivity of the charge-transfer excited state of the isolated titanium oxide species in tetrahedral coordination, $[Ti^{3+}-O^{-}]$.

6. 1. 2 Summary of Chapter 3

UV-irradiation of the highly dispersed titanium oxide catalysts in the presence of CO_2 and H_2O at 275 K led to formation of CH_4, CH_3OH, C_2-compounds, CO and O_2. The yield of the photocatalytic reaction strongly depended on the types of catalysts, the ratio of CO_2/H_2O and the reaction temperature. The photocatalytic reeducation of CO_2 with H_2O is linked to the much higher reactivity of the charge transfer excited state, i.e., $(Ti^{3+}\text{-}O^{-})$ of the tetrahedral coordinated titanium oxide species formed on the surfaces. Based on the detection of the reaction intermediate species such as Ti^{3+}, H atoms, and C radicals, a molecular scale reaction mechanism has been proposed. Titanium-silicon (Ti/Si) binary oxides prepared by the sol-gel method with different Ti contents exhibit high photocatalytic reactivity for the reduction of CO_2 with H_2O to form CH_4 and CH_3OH. A dramatic enhancement in the photocatalytic reactivity was found in regions of lower Ti content.

6. 1. 3 Summary of Chapter 4

Using the F^- media the hydrophobic zeolite and mesoporous silica can be synthesized. These hydrophobic porous materials exhibit the high ability for the adsorption of organic compounds diluted in water and become

the useful supports of photocatalyst. The hydrophobic Ti-Beta(F) zeolite prepared in the F^- media exhibited highly efficiency than the hydrophilic Ti-Beta(OH) zeolite prepared in OH^- media for the liquid-phase photocatalytic degradation of 2-propanol diluted in water to produce CO_2 and H_2O. The TiO_2 loaded on the hydrophobic mesoporous silica HMS(F) (TiO_2/HMS(F)), which was synthesized using tetraethyl orthosilicate, tetraethylammonium fluoride as the source of the fluoride and dodecylamine as templates, also exhibited the efficient photocatalytic performance for the degradation. The amount of adsorption of 2-propanol and the photocatalytic reactivity for the degradation increased with increasing the content of fluoride ions on these photocatalysts. The efficient photocatalytic degradation of 2-propanol diluted in water on Ti-Beta(F) zeolite and TiO_2/HMS(F) mesoporous silica can be attributed to the larger affinity for the adsorption of propanol molecules on the titanium oxide species depending on the hydrophobic surface properties of these photocatalysts.

6. 1. 5 Summary of Chapter 5

TiO_2 photocatalysts were synthesized by a hydrothermal method from tetraisopropyl orthotitanate (TPOT) in the presence of NH_4F with different NH_4F/Ti molar ratios (0, 0.25, and 1). The formation of well-crystallized anatase phase of TiO_2 and suppression of phase transition to rutile were observed even at high calcination temperature as the effects of presence of NH_4F. The TiO_2 hydrothermal synthesized with NH_4F

exhibited the absorption with a shift to the longer wavelength of visible-light region. The hydrothermal synthesized TiO_2 with moderate amount of NH_4F exhibited high photocatalytic activity for the degradation of alcohol diluted in water under both UV-light and visible-light irradiation.

6. 2 General Conclusions

Summarizing the results of each chapter, the following conclusions can be drawn;

[1] Titanium-Silicon (Ti/Si) binary oxides having different Ti contents showed dramatically enhanced photocatalytic reactivity for the liquid-phase oxidation of 1-octanol to 1-octanal in regions of lower Ti content. In the hydrogenation and hydrogenolysis of CH_3CCH with H_2O, the hydrogenolysis reaction (C_2H_6 formation) was predominant in regions of low Ti content, while the hydrogenation reaction (C_3H_6 formation) proceeded in redions of high Ti content. In situ photoluminescence, UV-vis reflectance, FT-IR, ESR, XAFS, XRD, and XPS spectroscopic investigation of these Ti/Si binary oxides indicated that the titanium oxide species are highly dispersed in the SiO_2 matrixes and exist in a tetrahedral coordination.

[2] UV-irradiation on the highly dispersed titanium oxide catalysts in the presence of CO_2 and H_2O at 275 K led to formation of CH_4, CH_3OH, C_2-compounds, CO and O_2. The yield of the photocatalytic reaction strongly depended on the types of catalysts, the ratio of CO_2/H_2O and the reaction temperature. The photocatalytic reduction of CO_2 with H_2O is linked to the much higher reactivity of the charge transfer excited state, i.e., $(Ti^{3+}\text{-}O^{-})$ of the tetrahedral coordinated titanium oxide species formed on the surfaces.

[3] The hydrophobic Ti-Beta(F) zeolite prepared in the F^- media exhibited high efficiency than the hydrophilic Ti-Beta(OH) zeolite prepared in OH^- media for the liquid-phase photocatalytic degradation of 2-propanol diluted in water to produce CO_2 and H_2O. The TiO_2 loaded on the hydrophobic mesoporous silica also exhibited the efficient photocatalytic performance for the degradation. The amount of adsorption of 2-propanol and the photocatalytic reactivity for the degradation increased with increasing the content of fluoride ions on these photocatalysts. The hydrophobic mesoporous surface is suitable as the photocatalytic reaction field for the degradation of organic compounds diluted in water.

[4] TiO_2 photocatalysts synthesized by a hydrothermal method in the presence of NH_4F had well-crystallized anatase phase of TiO_2 and suppression of phase transition to rutile were observed even at high calcination temperature as the effects of presence of NH_4F. The TiO_2

hydrothermally synthesized with NH_4F exhibited the absorption with a shift to the longer wavelength of visible-light region and high photocatalytic activity for the degradation of alcohol diluted in water under both UV-light and visible-light irradiation.

Acknowledgement

The author, Shinichi Kawasaki, expresses his sincerest gratitude to his supervisor, Professor Hiromi Yamashita of the Division of Materials and Manufacturing Science, Graduate School of Engineering, Osaka University for his constructive guidance, fruitful discussions and kind encouragement throughout this study. Sincere thanks are extended to Professor Toshihiro Tanaka and Professor Shinji Fujimoto of Osaka University for their critical reading of this thesis and their helpful comments for its improvement. He acknowledges the support of Associate Professor, Iwao Katayama, Assistant Professor, Kosuke Mori, Assistant Professor, Takeshi Kamegawa and Technical Stuff, Tetsutaro Ohmichi, for their instructive discussions, suggestions and continual encouragement through out this work.

The author wishes to thank Professor Masakazu Anpo and Associate Professor Masaya Matsuoka of Osaka Prefecture University and Assistant Professor Yuichi Ichihashi of Kobe University, for their supervising suggestions and constructive guidance during this work.

Finally, the author thanks his family for their understanding and strong encouragement towards his research work.

December, 2008

Shinichi Kawasaki

List of Publications Related to This Thesis

1) H. Yamashita, A. Shiga, S. Kawasaki, Y. Ichihashi, S. Ehara, M. Anpo
"Photocatalytic Synthesis of CH_4 and CH_3OH From CO_2 and H_2O on Highly Dispersed Active Titanium Oxide Catalysts."
Energy. Conv. Manag., **36**, 617-620 (1995).

2) 安保正一、山下弘巳、河崎真一、市橋祐一
「酸化チタンを光触媒とする二酸化炭素の水による還元固定化」
石油学会誌、**38**, 300-310 (1995).

3) H. Yamashita, S. Kawasaki, Y. Fujii, Y. Ichihashi, S. Ehara, S. E. Park, J. S. Chang, J. W. Yoo, M. Anpo
"Photocatalytic Reduction of CO_2 with H_2O on Ti/Si Binary Oxide Catalysts Prepared by the Sol-Gel Method."
Stud. Surf. Sci. Catal., **114**, 561-564 (1998).

4) H. Yamashita, S. Kawasaki, Y. Ichihashi, M. Takeuchi, M. Harada, M. Anpo, C. Louis, M. Che
"Characterization of Ti/Si Binary Oxides Prepared by the Sol-Gel Method and Their Photocatalytic Properties: The Hydrogenation and Hydrogenolysis of CH_3CCH with H_2O"
Koran J. Chem. Eng., **15**, 491-495 (1998)

5) H. Yamashita, S. Kawasaki, Y. Ichihashi, M. Harada, M. Anpo, G. Stewart, M. A. Fox, C. Louis, M. Che
"Characterization of Titanium-Silicon Binary Oxide Catalysts Prepared by the Sol-Gel Method and Their Photocatalytic Reactivity for the Liquid Phase Oxidation of 1-Octanol ."
J. Phys. Chem. B, **102**, 5870-5875 (1998).

6) S. Kawasaki, Y. Okada, S. Yuan, K. Mori, H. Yamashita
"Photocatalytic Degradation of Organics Diluted in Water Using TiO_2 Loaded on Fluoride-Modified Mesoporous Silica"
Mat. Sci. Forum., 544-545, 115-118 (2007).

7) H. Yamashita, S. Kawasaki, S. Yuan, K. Maekawa, M.Anpo, M. Matsumura
"Efficient Adsorption and Photocatalytic Degradation of Organic Pollutants Diluted in Water Using the Fluoride-modified Hydrophobic Titanium Oxide Photocatalysts: Ti-containing Beta Zeolite and TiO_2 Loaded on HMS Mesoporous Silica"
Catal. Today, **126**, 375-381 (2007).

8) S.Kawasaki, K. Maki, S. Yuan, Y. Matsumura, K. Mori, and H.Yamashita
"Degrdadation of Organic Compounds on TiO_2 Photocatalysts Prepared by Hydrothermal Method in the Presence of NH_4F"
Res. Chem. Intermed., in press.

List of Other Publications

1) S. Yuan, S. Okada, K. Maki, Y. Kuwahara, M. Tomonari, S. Kawasaki, K. Mori, H. Yamashita

"Synthesis and Photocatalytic Activity of TiO_2 Nanoparticles Loaded on the Fluorine-modified Hydrophobic Mesoporous Silica"

Solid State Phenomena, **124-126**, 1817-1820 (2007).

2) Y. Nishida, S. Kawasaki , S. Yuan, K. Mori , M. Narisawa, Y. Matsumura, T. Ohmich, I. Katayama, H. Yamashita

"Application of TiO_2 Photocatalyst Deposited on SiC for Degradation of Organic Compounds Diluted in Water"

Adv. In Tch. of Mat. Proc. J. (ATM), Advances in Technology of Materials and Materials Processing Journal (ATM), 9, 59-62 (2007).

3) S. Yuan, S. Kawasaki, K. Mori, H. Yamashita

"Synthesis and Photocatalytic Activity of TiO_2 Nanoparticles Fluorine-modified with TiF_4"

*Res. Chem. Intermed.,*34, 331-337 (2008).